SYNTHESIS AND BIOLOGICAL EVALUATION OF AROMATIC ENONES AND DIENONES RELATED TO CURCUMIN

by

RICHARD B. HUBBARD IV

(Under Direction the of Dr. J. Phillip Bowen)

ABSTRACT

Curcumin, a natural product isolated from the spice turmeric, has been shown to exhibit a wide range of pharmacological activities including certain anticancer properties. It has been specifically shown to be an effective inhibitor of angiogenesis both *in vitro* and *in vivo*. Using curcumin as a lead compound for antiangiogenic analog design, a series of structurally related compounds utilizing a substituted enone and dienone backbone have been synthesized and tested via an established SVR cell proliferation assay. The results have yielded a wide range of compounds that equal or exceed curcumin's ability to inhibit endothelial cell growth *in vitro*. Due to both their commercial availability and their fairly straight forward synthetic preparation, these low molecular weight compounds are attractive leads for developing future angiogenic inhibitors.

INDEX WORDS: Curcumin, Chalcone, Enone, Dienone, Angiogenesis, Cancer, Tumor

SYNTHESIS AND BIOLOGICAL EVALUATION OF AROMATIC ENONES AND DIENONES RELATED TO CURCUMIN

by

RICHARD B. HUBBARD IV

B.S., Furman University, 1995

M.S., Furman University, 1998

A Dissertation Submitted to the Graduate Faculty of The University of Georgia in Partial Fulfillment of the Requirements for the Degree

DOCTOR OF PHILOSOPHY

ATHENS, GEORGIA

2005

SYNTHESIS AND BIOLOGICAL EVALUATION OF AROMATIC ENONES AND DIENONES RELATED TO CURCUMIN

by

RICHARD B. HUBBARD IV

Major Professor: Dr. J. Phillip Bowen

Committee: Dr. Will Taylor
Dr. Robert S. Phillips

Electronic Version Approved:

Maureen Grasso
Dean of the Graduate School
The University of Georgia
May 2005

DEDICATION

To my parents, Richard and Janet and my sister, Elizabeth, for all of their love, patience and support over the years.

ACKNOWLEDGEMENTS

I would like to thank Tedman Elhers, Karl Kirshner, Phil Robinson, Jennifer Sorensen, Patt Methe, Peggy Norman and Eric Gapud for their time, friendship and patience during my journey through the University of Georgia's Doctoral program. Without their help, my experiences here at UGA would not have been as educational or enjoyable.

I would like to offer a special thanks to the members of my graduate committee, Dr. Will Taylor and Dr. Robert Phillips. Thank you for your guidance and support. Last, but not least, I would like to thank my advisor, Dr. J. Phillip Bowen. Thank you for your faith in my abilities and providing me with a fascinating research project to participate in during my time in Athens.

TABLE OF CONTENTS

Page

LIST OF TABLES

Page

LIST OF FIGURES

Page

CHAPTER 1

INTRODUCTION

Cancer and Angiogenesis

Cancer is a general term used to describe a variety of diseases characterized by the abnormal and uncontrolled proliferation of cells. During the normal process of cell differentiation, biological control mechanisms set parameters for cellular growth and division. Contact inhibition is one of these control mechanisms. When developing cells become crowded together, contact between their outer surfaces begin to repress cell movement and division.[1] Through contact inhibition, the genes which control cell division are rendered inactive. A cancer cell, by definition, is a cell which has somehow evaded the effects of contact inhibition and other cellular controls essential to the regulation of cell growth and division. As these cancer cells differentiate, a mass known as a tumor begins to form. Without the normal biological regulations of growth and cell mortality, cancerous cells become essentially immortal. The resulting neoplasms can invade and destroy surrounding normal tissue. Cancerous cells can then spread or metastasize from the primary tumor site throughout the blood and lymphatic system to develop new cancers in remote parts of the body.

The current treatment options available to patients suffering from aggressive forms of cancer are divided into three main categories: surgical intervention, radiation therapy, and chemotherapy. As the name implies, surgical intervention involves the physical removal of the cancerous mass from the patient's body. This is a highly invasive procedure that is not always completely effective. In addition, not all patients are suited to endure the rigors of surgery

depending on the advancement of the disease. Whereas the main body of the tumor may be successfully excised, metastases located in remote areas of the body will not be removed and can therefore continue to cause problems (remission). Radiation therapy utilizes ionizing energy to damage and ultimately kill cancer cells. External radiation therapy is the use of a machine to focus high-energy emissions at the tumor mass. Internal radiation therapy is the placement of radioactive material inside the body as close as possible to the cancer source in an effort to eradicate it. While radiation can be an efficient, noninvasive means of killing cancerous cells, it also results in various deleterious side effects such as nausea, hair loss, systemic cell death, and even the possibility of additional carcinogenesis. The final treatment alternative is chemotherapy. This technique utilizes cytotoxic agents that are introduced into the body and specifically seek out the tumor mass in order to cause sufficient cellular damage to result in the eventual death of the tumor. Like radiation therapy, chemotherapy is a noninvasive technique. It does, however, possess many of the same harmful side effects. Drug specificity is improving, but in many cases a significant number of healthy cells are killed along with the cancerous ones. In an effort to provide novel and systemically sound treatment options for long suffering cancer patients, new avenues of cancer prevention and eradication are being investigated everyday. One of the most promising new ways of halting the progression of cancer is through the manipulation of angiogenesis.

Angiogenesis is defined as the growth and development of new blood vessels, a process that occurs in healthy individuals in relation to the healing of wounds, embryonic development, restoration of blood flow to ischemic tissues, and the menstrual cycle in females. In mature adults, it is typically a quiescent or tightly regulated process. Angiogenesis is typically initiated by a shift in the normal balance of endogenous inhibitors and promoters. In disease states such

as cancer, however, the body loses the ability to sustain balanced angiogenesis. New blood vessels form at abnormal rates and often end up sustaining diseased tissue (tumors), damaging normal tissue, and even allowing tumor cells to escape into the circulation, resulting in metastases. Additional disease states that rely on abnormal angiogenic activity are rheumatoid arthritis[2] and diabetic retinopathy.[3]

Dr. Judah Folkman pioneered the field of angiostatic therapy in the early 1970's.[4,5] He discovered that developing tumors must undergo neovascularization in order to provide themselves with a source of nutrients and a means of excreting waste materials. In order for an existing tumor mass to grow larger than 1-2 mm in size it must develop its own independent blood supply. The key to angiogenesis is the stimulated proliferation of the endothelial cells that line the insides of the body's capillaries. As such, if one could develop a treatment that was capable of suppressing the proliferation of these same endothelial cells, the abnormal formation of new blood vessels would be curtailed and consequently, the cancerous mass would effectively be starved to death. Because angiogenesis is normally a quiescent natural process, the potential side effects of this form of therapy are considered to be negligible. In theory, there should be no systemic cell death or abnormal side effects associated with a treatment regime that simply aims to regulate a largely inactive bodily process. Angiogenesis inhibitors represent a new class of drugs targeted against the abnormal up regulation of angiogenesis in an effort to block or slow tumor growth. The current project is based on the design, synthesis, and biological evaluation of just such a class of compounds. Enone and dienone derivatives of the natural spice curcumin have been synthesized and evaluated in regards to their antiangiogenic properties. The project background and the collected data are presented for inspection in the following chapters of this manuscript.

Curcumin and Proposed Enone/Dienone Derivatives

Curcumin, also known as diferuloylmethane, is a carotenoid pigment isolated from the spice turmeric. Its molecular structure is provided in Figure 1. Turmeric itself is originally obtained from the powdered rhizome of the plant Curcuma longa L.[6,7] Curcumin is the major bioactive component of turmeric and it has been shown to exhibit a wide range of interesting biological activities. These include antioxidant,[8,9] anti-inflammatory,[10,11] and anti-HIV properties.[12,13] Perhaps most importantly, it has also exhibited significant antitumor activity. Curcumin has been shown to inhibit the progression of artificially induced skin and colon cancers effectively in animal models.[14-18] Both of these forms of cancer differ significantly in their genetic basis, which has lead researchers to postulate that curcumin's ability to hinder their progression is based on its effectiveness as an inhibitor of angiogenesis. Dr. Jack Arbiser and coworkers at Emory University, have subsequently found that curcumin is in fact able to inhibit basic fibroblast growth factor (bFGF)-induced endothelial cell proliferation *in vitro* and does, in fact, inhibit angiogenesis *in vivo*.[19]

Although the specific mechanism by which curcumin enacts its inhibition of the angiogenic process is not currently known, its efficacy in doing so, coupled with its relatively straightforward chemical structure, have made it an attractive lead compound for structure modification and drug development studies. The current synthetic efforts of the Bowen research group have centered primarily on the modification of the central region of the molecule. The hepta-1,6-dien-3,5-dione linker has been shortened to a more compact enone or dienone backbone. This, coupled with modifications to the size and substitution patterns of the two aromatic ring moieties present in the molecule, has yielded a number of highly effective curcumin analogs which show impressive anti-proliferative activity toward SVR endothelial cells

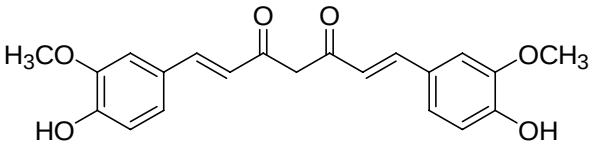

Figure 1. Structure of Curcumin

in vitro.[20-22] A detailed account of these compounds and their corresponding biological activities will be provided in this manuscript.

It has been proposed that the biological efficacy of curcumin arises from the electrophilic nature of its central β-diketone component.[20,21] Each of the two separate enone moieties present in curcumin's linker region theoretically allows for the possibility of covalent bond formation via a 1,4 Michael addition. It is currently unknown whether or not covalent interaction within a unique active site is the principal mechanism of curcumin's observed antiangiogenic activity. The ongoing project described in this document was primarily designed to investigate this theory and provide additional data by which a more fully formed explanation could be elucidated. Toward this end, each of the aromatic enone and dienone derivatives selected for synthesis and biological evaluation retain this essential electrophilic moiety, while at the same time, the overall structure of the molecule is simplified to aid in both the ease of general analog synthesis and the implementation of various aromatic moiety modifications. In an effort to develop a robust pharmacophoric model in the hopes of better understanding the basis for its' biological activity, the structure of curcumin was subdivided into three key regions of interest: two substituted aromatic moieties (A and C) joined together by the conjugated β-diketone linker (B) [see Figure 2].

After dividing the molecule into three specific, modifiable regions, two simple, yet effective, pharmacophore models for the design and synthesis of novel curcumin analogs were

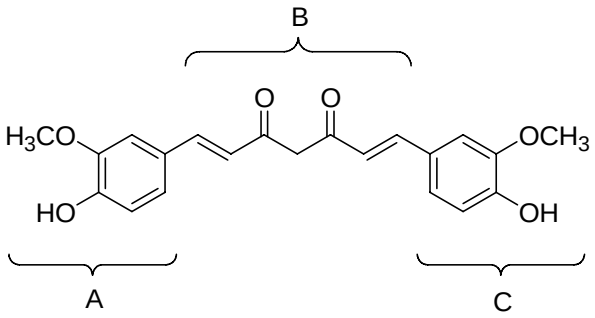

Figure 2. Key Structural Regions of Curcumin

developed. Each individual region could be modified independently of the others in order to aid in the systematic refinement of the search for increasingly effective antiangiogenic inhibitors. In the current study, compounds with an abbreviated linker located between the two terminal aromatic regions comprised the primary focus. The linker (B) was shortened from curcumin's original β-diketone to one of three more compact, but equally electrophilic structures. The three primary linker modifications investigated in this study were: 1. a single enone moiety (propenone), 2. a penta-1,4-dien-3-one group or 3. a 2,6-dimethylenecycloalkanone. The modified linkers are designated as B' in Figures 3 and 4. Working within this new molecular framework (A′,B′,C′), a variety of mixed aromatic systems and substitution patterns were either obtained from commercial sources or synthesized in the laboratory. Figures 3 and 4 are generalized representations of the pharmacophore substitution patterns investigated to date and for which biological data is presented in the current document. Each compound's biological efficacy as an *in vitro* inhibitor of endothelial cell proliferation, and thus potentially angiogenesis, was evaluated via an established SVR cell assay developed by the collaborating dermatology laboratory at Emory University run by Dr. Jack Arbiser, MD, PhD. Dr. Arbiser created the SVR cell line while working with Dr. Judah Folkman at Harvard Medical School in 1997. More detail will be provided concerning the general procedures of the SVR endothelial

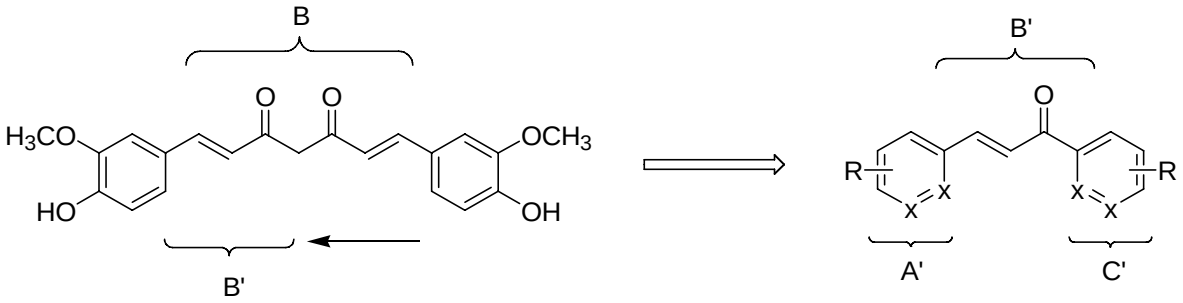

Figure 3. Generalized Representation of the Linker Modification and Substitution Patterns of the Aromatic Enone Analogs. R=Cl, F, CH_3, NO_2, isopropyl, OBn, phenyl, OCH_3, OH; X=C, N; A' & C' = benzene, pyridine, furan, pyrrole, naphthalene, anthracene, biphenyl, 5-benzo[1,3]dioxole.

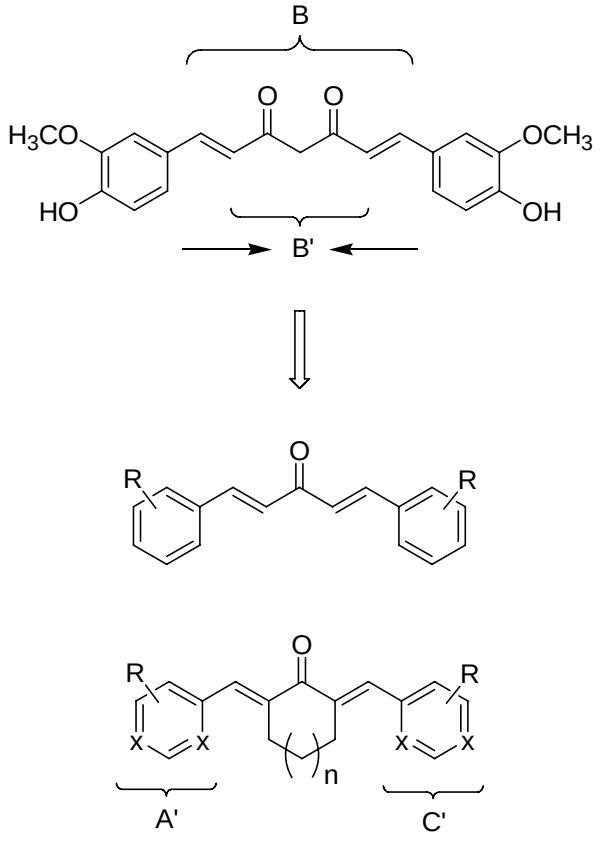

Figure 4. Generalized Representation of the Linker Modification and Substitution Patterns of the Aromatic Dienone Analogs. R=Cl, F, OCH_3, OH, $N(CH_3)_2$; n=0,1; X=C, N; A' & C' = benzene, pyridine, furan, pyrrole, naphthalene, anthracene, 5-benzo[1,3]dioxole.

cell assays in the following chapter. Curcumin has previously been shown to inhibit *in vitro* SVR endothelial cell growth by 41.5% at 1 ug/mL, 37.8% at 3 ug/mL, and 56.2% at 6 ug/mL. These values were used as a general benchmark by which to judge the relative effectiveness of the synthesized derivatives. Analogs scoring comparable or higher values than those of curcumin were deemed a success.

The curcumin derivatives synthesized for the purposes of this study were prepared via a series of Claisen-Schmidt Condensations.[23] The condensation of an aromatic aldehyde with an aliphatic ketone in the presence of a relatively strong base (sodium or potassium hydroxide) yields an α,β-unsaturated ketone product. The enone derivatives presented herein were the result of a reaction between the appropriate aromatic aldehydes and various arylmethyl ketones. The dienone analogs were synthesized using those same aldehydes coupled with either acetone or cyclohexanone. The trans isomers of the resulting α,β-unsaturated ketone products were obtained exclusively. This was determined via melting point values for compounds that had been previously characterized in the literature, in addition to ^{1}H NMR data analysis (j coupling values).

CHAPTER 2

SVR CELL STUDIES

Overview and Experimental Design

As previously stated, the immortalized endothelial cell proliferation assays used in this study were developed by Arbiser *et al.* at Harvard University.[24] Primary murine (mouse) endothelial cells, collected from the pancreatic islets of adult, inbred C57BL/6 mice, were first infected with an ecotropic retrovirus encoding the simian virus 40 (SV-40) large T antigen (58-3 allele) in addition to neomycin resistance.[25] The retrovirus will only infect and replicate in cells from the original host species, in this case, mouse. Neomycin is a broad spectrum aminoglycoside antibiotic and antibacterial agent. It is highly toxic to cells and that toxicity, coupled with the newly encoded resistance, can subsequently be used to cull the non-transfected cells from the successfully transfected ones. In this case, however, the resulting cells were selected in a solution of Dulbecco's modified eagle's medium (DMEM), 5% fetal calf serum and 0.6 mg/mL geneticin sulfate (G-418). Geneticin sulfate is an aminoglycoside antibiotic similar in structure to neomycin and is used in its place to eradicate the non-transfected cells. The cloned cells were then stained with 1,1′-dioctadecyl-3,3,3′,3′-tetramethylindocyanine perchlorate coupled to acetylated, low density lipoprotein (diI-Ac-LDL).[26] Fluorescence microscopy was used to identify the positive clones. The specific clone designated MS1 was expanded and infected with an additional retrovirus which encoded for both activated H-*ras* and hygromycin resistance.[27,28] The H-*ras* allele introduced by the retrovirus contained mutations at glycine-12 and threonine-59.[28] The cells were then washed with a 50 μg/mL solution of hygromycin in

order to isolate the newly transfected cells. The resulting, immortalized endothelial cell line was given the designator SVR. The inclusion of the simian virus 40 accounts for the "SV" portion of the nomenclature, while the "R" is gleaned from the inclusion of activated H-*ras*.

For their use in the *in vitro* assays, the SVR cells were plated 10,000 cells/well in a 24 well cell culture dish (see Figure 5). The cells were initially cultured for one day at 37°C in 10% DMEM (1 mL/well) under a 5.0 - 5.2% CO_2 atmosphere. During the first 24 hour incubation period, the living cells adhered to the bottom of their individual wells. The DMEM growth media was then aspirated and replaced with 0.5 mL of a fresh 10% DMEM solution containing 1, 3, 6, or 9 μg/mL concentrations of the individual test compounds. Each drug was dissolved in a minimal amount of dimethylsulfoxide (DMSO) in order to prepare stock test solutions (10 mg/mL) from which the appropriate drug dilutions were obtained. For this reason, each plate utilized one column (4 wells) as a DMSO control group for each specific drug concentration tested in the assay. A single microliter of each individual stock solution was added to 1 mL of fresh growth medium resulting in a 10 μg/mL solution. Subsequently, 0.1, 0.3, 0.6, and 0.9 mL of these solutions were then added to an additional 0.9, 0.7, 0.4, and 0.1 mL aliquots of 10% DMEM, respectively, in order to generate the appropriate individual drug concentrations required for testing. After the addition of the drug solutions, the cell culture plates were allowed to incubate for an additional 48 hours under identical conditions used during the initial incubation period. At the end of the two day period, each of the wells was aspirated and then washed with 0.5 mL of Dulbecco's Phosphate Buffered Saline (DPBS) and aspirated again in order to remove any dead cells or lingering DMEM. The remaining, live cells were removed from the bottom of each well using 0.5 mL of a 1X trypsin-EDTA solution (0.25% trypsin, 2.21 mM EDTA in HBSS without Ca, Mg, or $NaHCO_3$). The occasional agitation and microscopic

examination of the culture plate gave sufficient evidence of complete cell detachment. The enzymatic activity of the trypsin was then neutralized with the addition of 0.5 mL of fresh 10% DMEM after approximately 8 minutes. After each well was thoroughly mixed to insure homogeneity, 0.5 mL of the media from each well was extracted and mixed with 9.5 mL of Coulter's Isoton II balanced electrolyte solution and the total number of cells/well were counted using a Beckman Coulter Z1 cell and particle counter. The total cell count for each test well was then compared to the DMSO control well for each respective drug concentration. The percent inhibition of cell growth was calculated from these values.

	Compound 1	**Compound 2**	**Compound 3**	**Compound 4**	**Compound 5**	**Control**
1 µg/mL	Well 1	Well 5	Well 9	Well 13	Well 17	Well 21
3 µg/mL	Well 2	Well 6	Well 10	Well 14	Well 18	Well 22
6 µg/mL	Well 3	Well 7	Well 11	Well 15	Well 19	Well 23
9 µg/mL	Well 4	Well 8	Well 12	Well 16	Well 20	Well 24

Figure 5. Representation of a Typical SVR Cell Culture Plate

Experimental Procedure

All of the cell work reported in the following experimental section was performed in a Class II A/B3 biological safety cabinet from Forma Scientific. UV illumination and positive airflow were used in conjunction with frequent ethanol wipe downs to ensure a sterile work environment. No reagent bottles or cell culture plates/flasks were opened outside of the confines of the hood to avoid possible contamination. The only exceptions to this rule were cell culture plates that had been washed with the trypsin-EDTA solution in preparation for a final cell count. At this point, sterility became unnecessary.

The cell counts were performed using a dual threshold Coulter Z1 cell and particle counter with 1 – 120 micron range. The counter threshold was set for 5 μm cell diameters, but was capable of detecting sizes slightly above and below the programmed set point in order to take into account any possible cell deformation experienced as a result of the trypsin-EDTA wash. The particle counter utilizes the "Coulter Principle" to estimate the number of cells present in an electrolyte solution and is the recommended limit test for particulate matter in parental solutions. It is based on measurable changes in electrical resistance produced by nonconductive particles suspended in an electrolyte solution. A small aperture located between a pair of electrodes housed within the counter's probe comprises the sensing zone that the suspended particles pass through. While inside the probe, each particle displaces a specific volume of fluid which is measured as a voltage pulse where the height measured is proportional to the particle's volume. The solution quantity drawn through the probe is precisely controlled to allow the apparatus to count the number of particles present in a specific volume of fluid (0.5 mL). Several thousand particles per second can be counted using this method which is independent of particle shape, color and density.

The growth media used in the reported cell assays was formulated in a Corning Incorporated (Costar #430770) 500 mL filtration system. It consists of a mixing flask and a catch flask each composed of non-pyrogenic polystyrene and separated by a 0.45 μm cellulose acetate, low protein binding membrane. The presence of the filtering membrane ensures the sterility of the final growth media solution by excluding any harmful bacteria or viruses. In the mixing flask, 436 mL of pure Dulbecco's modified eagle's medium (with 1000 mg glucose/L, L-glutamine, $NaHCO_3$ and pyridoxine·HCl) was combined with 7 mL of a sterile antibiotic/antimycotic solution containing 10,000 units of penicillin, 10 mg of streptomycin and

25 μg/mL of amphotericin B. The resulting solution was continually stirred as 7 mL of a 200 mM (29.20 mg/mL) solution of L-glutamine and 50 mL of sterile fetal bovine serum (mycoplasma, virus and endotoxin tested) was added. The mixture was then passed through the filtering membrane into the catch flask under vacuum, resulting in a 10% DMEM solution (based on fetal bovine serum volume).

Once the growth media was prepared, a small portion of immortalized endothelial cells was obtained from cold storage (liquid nitrogen temperatures) and multiplied for use in the SVR assays. A 75 cm^2 Corning Incorporated (Costar #3376) cell culture flask (T75) made from treated, non-pyrogenic polystyrene was charged with several thousand cells and 10 mL of 10% DMEM. The flask was fitted with a 0.2 μm vent cap to allow the influx of CO_2 and then placed in a Nuaire US autoflow incubator. The incubator used was water jacketed and HEPA filtered to ensure a controlled and sterile environment. The cells were incubated for approximately 24 - 48 hours under a 5.0 – 5.2% CO_2 atmosphere at 37°C. During the initial incubation period the cells were checked periodically to monitor their status and to check for confluence. Once 50 – 100% (typically 70-80%) coverage was observed, the cells were then prepared for collection. The growth media was aspirated from the flask and the cells adhered to the vessel's surface were then washed with Dulbecco's phosphate buffered saline (DPBS with calcium and magnesium) in order to separate and remove any remaining dead cells. The wash also removed any residual DMEM, which is known to interfere with the enzymatic activity of trypsin. At this stage, 1 mL of trypsin-EDTA was added in order to separate the cells from the bottom of the flask. The solution was allowed to stand for approximately 1-2 minutes, while frequent checks were made to ensure that the cells were indeed detaching from the floor of the flask. At this point the trypsin-EDTA and cell mixture was homogenized using a 5 mL pipet and transferred into a

sterile 15 mL polystyrene centrifuge tube. The trypsin-EDTA solution (1 mL) was then combined with 9 mL of fresh 10% DMEM media and homogenized again. The number of cells present in the resulting mixture was determined by removing 0.5 mL of the solution, mixing it with 9.5 mL of Coulter's Isoton II balanced electrolyte solution and evaluating the number of cells using the Coulter Z1 particle counter. The solution was mixed and measured in a CMS Labcraft Accuvette II 35 mL vial. Using the data obtained from the cell count, the appropriate volume of stock solution containing approximately 10,000 SVR cells was then transferred into each individual well of a Corning Incorporated 24 well cell culture cluster (polystyrene), adjusted to 1 mL of total solution/well using fresh DMEM and allowed to incubate overnight in preparation for use in the SVR cell assays reported herein.

Results and Conclusions

The data tables provided in this chapter are divided into two main categories: 1. Total cell count statistics and 2. Percent SVR cell growth inhibition. These numbers are provided for the sake of completeness so that the reader is presented with all of the data collected during the course of the biological testing and will be able to reproduce the provided percent inhibition scores from the original cell count data obtained from each cell culture. The initial, raw cell count data was obtained from the Coulter Z1 cell and particle counter described previously. Remember that the flow of liquid through the counter's probe was limited to a specific volume (0.5 mL). Therefore, the value that was read from the counter's display represented approximately $1/20^{th}$ of the total cell count of the isoton/cell solution present in the accuvette. For this reason, the raw cell data was multiplied by 20 to generate the total SVR cell count for the individual test and control wells. The cell count data provided in the following tables has already been adjusted accordingly. The next step was to compare the total cell count for each

test well to the corresponding DMSO control well in order to calculate the percent cell growth inhibition exhibited by the individual compounds. The DMSO control well data for the compounds listed in Tables 1–14 has been provided in tabular form in Appendix A. The following formula was used to generate the percent inhibition values presented in this manuscript: (1-([test well cell count]/[control well cell count]))*100. 1,3-Diphenyl-propenone (**1**) is used as an example. The total SVR cell count for the 1 μg/mL concentration test well (48800 cells) is divided by the appropriate DMSO control well value located in Appendix A (171880 cells). The resulting number is then subtracted from one and multiplied by 100 to give the corresponding percent inhibition score of 71.6% located in Table 2.

All of the aromatic enone and dienone curcumin derivatives that have been synthesized and biologically evaluated by the Bowen laboratory are presented for inspection in this manuscript. They have been subdivided into appropriate groupings based on their general carbon backbone (enone/dienone) in addition to their specific aromatic moiety and linker region modifications. Tables 1-10 contain the various enone derivatives, while Tables 11-14 contain the dienone analogs. Within the general enone category, there exist five structural variations. Each structural grouping will be identified and analyzed as their specific data are presented. The first grouping of derivatives to be examined in this fashion is the standard enone analogs found in Tables 1-2 and Figures 6-7. These compounds are so named due to the structure of their linker region and the standard benzene aromatic moieties they contain. They possess a classic diphenylpropenone skeleton that most rigidly represents the enone pharmocophore model presented in the preceding chapter. The prototypical aromatic enone, chalcone (**1**), was the first enone analog tested and it was shown to inhibit SVR cell growth by 71.6% at 1 μg/mL, 92.8% at 3 μg/mL, and 94.4% at 6 μg/mL. This was a very encouraging data as it proved that even with

Table 1. Total Cell Count Data from *in vitro* SVR Cell Assays of Standard Enone Analogs

Compound	Total SVR Cell Count			
	1 µg/mL	3 µg/mL	6 µg/mL	9 µg/mL
1,3-Diphenylpropenone (1)	48800	10180	7160	----
1-(4-Chlorophenyl)-3-p-tolylpropenone (2)	120480	84560	53420	----
3-(2,6-Dichlorophenyl)-1-p-tolylpropenone (3)	45260	2620	2447	----
3-(2,4-Dichlorophenyl)-1-p-tolylpropenone (4)	137620	126720	19740	----
3-(4-Isopropylphenyl)-1-p-tolylpropenone (5)	138420	121300	52540	----
3-(2,6-Dimethylphenyl)-1-phenylpropenone (6)	89960	59460	13360	----
1,3-Di-p-tolylpropenone (7)	109480	46260	13460	----
1-(2,4-Dimethylphenyl)-3-phenylpropenone (8)	100280	27740	16400	----
3-(2-Chlorophenyl)-1-(2,4-dimethylphenyl)propenone (9)	120980	105680	34240	----
1,3-Di(4-chlorophenyl)propenone (10)	148240	124800	88680	----
3-Phenyl-1-(3-trifluoromethylphenyl)propenone (11)	99260	17880	3960	----
3-(4-Chlorophenyl)-1-p-tolylpropenone (12)	133560	106680	68820	----
1,3-Bis(2,6-dichloro-phenyl)propenone (13)	145100	69400	17640	5900
1-(4-Aminophenyl)-3-(3-aminophenyl)propenone (14)	889240	973680	486000	184360
1,3-Di(4-methoxyphenyl)propenone (15)	121900	51760	19100	----
3-(2,6-Dichlorophenyl)-1-phenylpropenone (16)	267540	109340	16900	3920
1-(2,6-Dichlorophenyl)-3-phenylpropenone (17)	99760	49860	11560	----
3-(2,6-Dichlorophenyl)-1-(2,6-dimethoxyphenyl)propenone (18)	137280	87200	67840	----
3-(2,6-Dimethoxyphenyl)-1-phenylpropenone (19)	121920	67480	55800	----
1-(2,6-Dimethoxyphenyl)-3-phenylpropenone (20)	132720	93240	51960	----
1,3-Bis(2,6-dimethoxyphenyl)propenone (21)	114080	78680	86480	----
1-Phenyl-3-pyridin-2-ylpropenone (22)	60540	11140	3160	----
1-Phenyl-3-pyridin-3-ylpropenone (23)	71160	69680	17100	----
1,3-Dipyridin-2-ylpropenone (24)	116320	47560	15120	----
1-Pentamethylphenyl-3-phenylpropenone (25)	156160	162880	134600	----
1-(4-carboxymethylphenyl)-3-phenylpropenone (26)	148260	136080	90480	----
1,3-Bispentafluorophenylpropenone (27)	----	----	----	----
3-(4-Nitro-phenyl)-1-phenylpropenone (28)	824280	467160	243400	88880
3-Pentafluorophenyl-1-phenylpropenone (29)	----	----	----	----
1-Pentafluorophenyl-3-phenylpropenone (30)	----	----	----	----
1,3-Diphenylpropan-1-one (31)	58220	61740	54280	28140
1,3-Diphenylpropynone (32)	277280	106840	13840	6440

Table 2. Percent Inhibition of *in vitro* SVR Cell Proliferation by Standard Enone Analogs

Compound	SVR Percent Growth Inhibition			
	1 µg/ml	3 µg/ml	6 µg/ml	9 µg/ml
1,3-Diphenylpropenone (1)	71.6	92.8	94.4	----
1-(4-Chlorophenyl)-3-p-tolylpropenone (2)	29.9	40.2	58.5	----
3-(2,6-Dichlorophenyl)-1-p-tolylpropenone (3)	73.7	98.2	98.1	----
3-(2,4-Dichlorophenyl)-1-p-tolylpropenone (4)	19.9	10.4	84.7	----
3-(4-Isopropylphenyl)-1-p-tolylpropenone (5)	19.5	14.2	59.2	----
3-(2,6-Dimethylphenyl)-1-phenylpropenone (6)	47.7	57.9	89.6	----
1,3-Di-p-tolylpropenone (7)	36.3	67.3	89.5	----
1-(2,4-Dimethylphenyl)-3-phenylpropenone (8)	41.7	80.4	87.3	----
3-(2-Chlorophenyl)-1-(2,4-dimethylphenyl)propenone (9)	29.6	25.3	73.4	----
1,3-Di(4-chlorophenyl)propenone (10)	13.8	11.7	31.1	----
3-Phenyl-1-(3-trifluoromethylphenyl)propenone (11)	42.3	87.4	96.9	----
3-(4-Chlorophenyl)-1-p-tolylpropenone (12)	22.3	24.5	46.5	----
1,3-Bis(2,6-dichlorophenyl)propenone (13)	22.0	79.6	92.0	98.4
3-(3-Aminophenyl)-1-(4-aminophenyl)propenone (14)	43.5	38.1	69.1	88.3
1,3-Di(4-methoxyphenyl)propenone (15)	29.1	63.4	85.2	----
3-(2,6-Dichlorophenyl)-1-phenylpropenone (16)	-43.7	67.9	92.4	99.0
1-(2,6-Dichlorophenyl)-3-phenylpropenone (17)	2.2	51.1	88.7	----
3-(2,6-Dichlorophenyl)-1-(2,6-dimethoxyphenyl)propenone (18)	23.2	43.7	52.3	----
3-(2,6-Dimethoxyphenyl)-1-phenylpropenone (19)	31.8	56.4	60.8	----
1-(2,6-Dimethoxyphenyl)-3-phenylpropenone (20)	25.8	39.8	63.5	----
1,3-Bis(2,6-dimethoxyphenyl)propenone (21)	36.2	49.2	39.2	----
1-Phenyl-3-pyridin-2-ylpropenone (22)	40.7	89.1	96.9	----
1-Phenyl-3-pyridin-3-ylpropenone (23)	30.3	31.7	83.2	----
1,3-Dipyridin-2-ylpropenone (24)	0.0	53.4	85.2	----
1-Pentamethylphenyl-3-phenylpropenone (25)	12.6	0.0	5.3	----
1-(4-carboxymethylphenyl)-3-phenylpropenone (26)	13.7	3.8	29.7	----
1,3-Dipentafluorophenylpropenone (27)	31.1	88.6	88.6	----
3-(4-Nitrophenyl)-1-phenylpropenone (28)	47.6	70.3	84.5	94.4
3-Pentafluorophenyl-1-phenylpropenone (29)	0.0	0.0	0.0	----
1-Pentafluorophenyl-3-phenylpropenone (30)	6.6	55.6	88.7	----
1,3-Diphenylpropan-1-one (31)	4.4	-1.8	18.9	50.6
1,3-Diphenylpropynone (32)	16.8	59.1	94.9	97.6

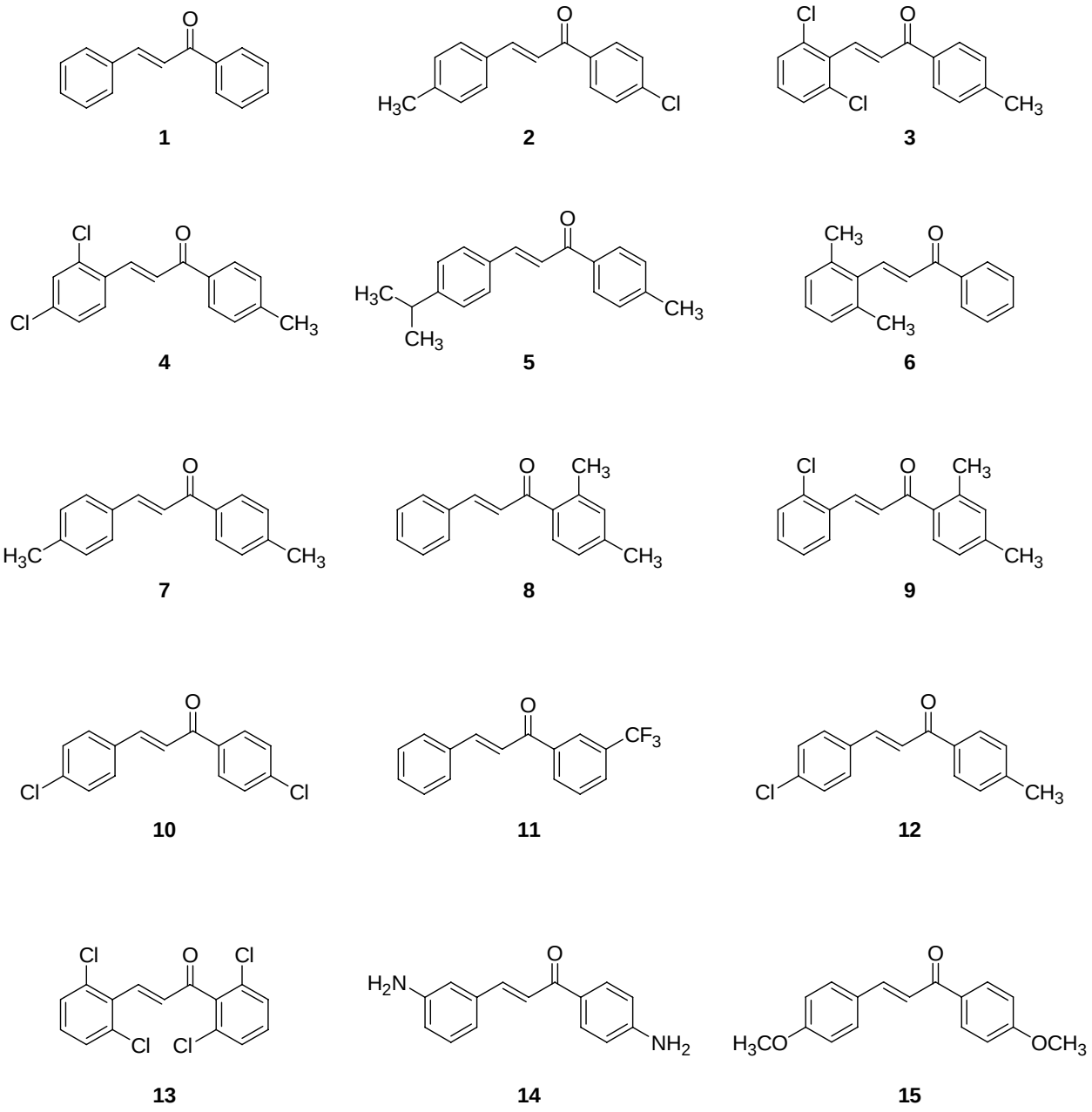

Figure 6. Structures of Compounds **1-15** from Tables 1 and 2

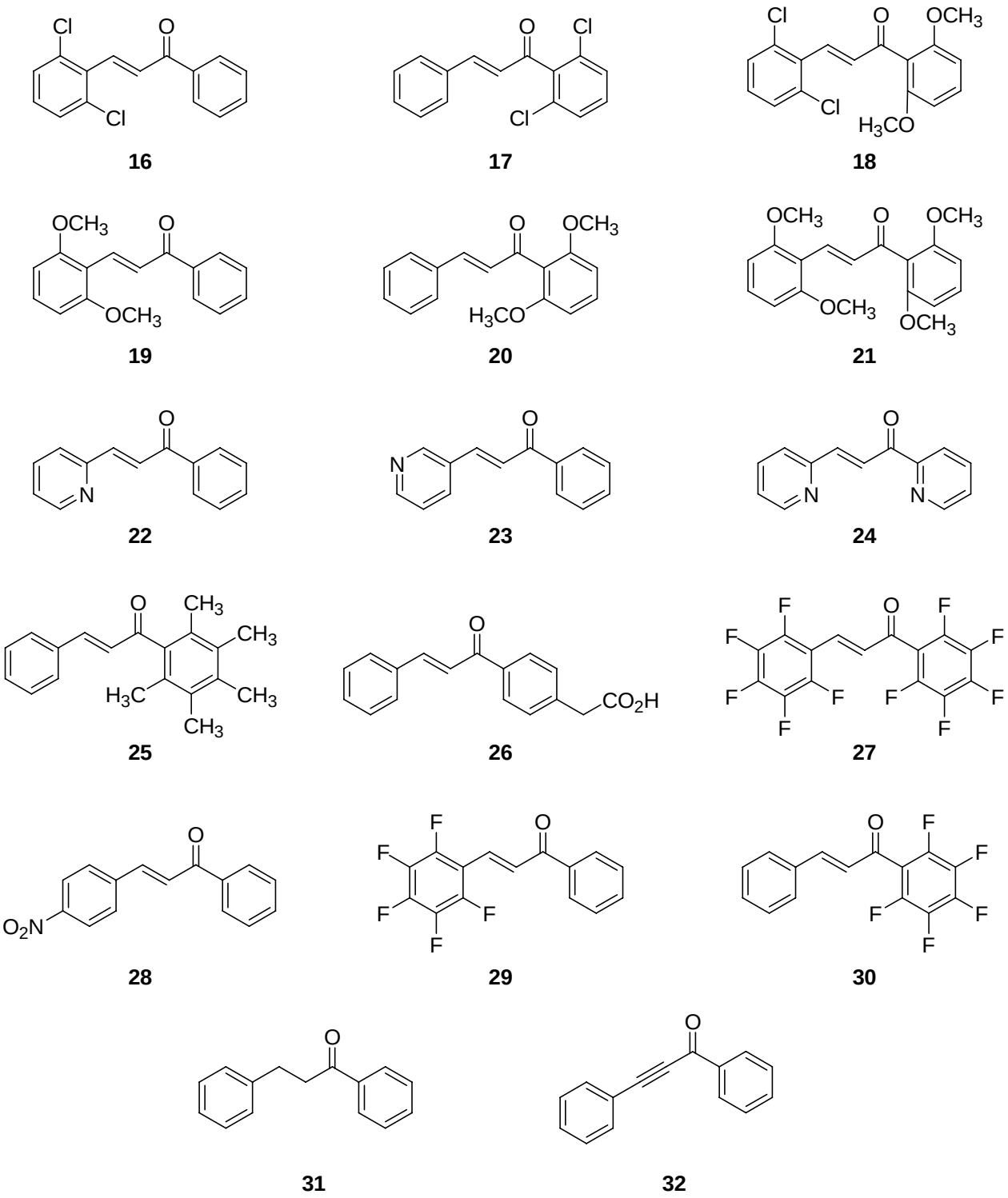

Figure 7. Structures of Compounds **16-32** from Tables 1 and 2

the simplified framework, the aromatic enone analogs still retain the fundamental structural characteristics required for biological potency. In fact, a significant number of the enone analogs investigated either matched or exceeded curcumin's levels of *in vitro* SVR cell growth inhibition.

In addition to chalcone, the 3-(2,6-Dichlorophenyl)-1-p-tolylpropenone derivative (**3**) also exhibited remarkable *in vitro* growth inhibition of the immortalized endothelial cells. It recorded 73.7%, 98.2% and 98.1% inhibition at concentrations of 1, 3 and 6 μg/mL. Compounds **1** and **3** are the most active standard chalcones synthesized to date. They demonstrate the highest levels of SVR inhibition at the lowest drug concentrations investigated. Numerous additional derivatives of this class show biological activity on par with curcumin at 1 μg/mL (41.5%), but then exceed its activity at higher concentrations (3-9 μg/mL). The purely alkyl substituted chalcones: 3-(2,6-Dimethylphenyl)-1-phenylpropenone (**6**), 1,3-Di-p-tolylpropenone (**7**), and 1-(2,4-Dimethylphenyl)-3-phenylpropenone (**8**) resulted in 36.3-47.7% inhibition at 1 μg/mL, 57.9-80.4% inhibition at 3 μg/mL, and 87.3-89.6% inhibition at 6 μg/mL (see Table 2). Additional derivatives containing various halogen substituents: 3-Phenyl-1-(3-trifluoromethylphenyl)propenone (**11**), 1,3-Bis(2,6-dichlorophenyl)propenone (**13**), and 3-(2,6-Dichlorophenyl)-1-phenylpropenone (**16**) resulted in lower activity at the 1 μg/mL (-43.7-42.3%) concentration, but comparable inhibition to compounds **6**, **7**, and **8** at 3 μg/mL (67.9-87.4%) and 6 μg/mL (92.0-96.9%). Two aromatic substitutions that were shown to inhibit successfully SVR cell growth were the additions of a pyridine ring in compound **22** (1-phenyl-3-(2-pyridyl)propenone) and a *para*-nitro group in compound **28** (3-(4-Nitrophenyl)-1-phenylpropenone). These nitrogen containing compounds resulted in percent inhibition results of 40.7-47.6% at 1 μg/mL, 70.3-89.1% at 3 μg/mL, and 84.5-96.9% at 6 μg/mL.

In addition to the standard propenone derivatives listed above, two additional compounds were included in Tables 1 and 2 for the purpose of general activity comparison. Compound **31**, 1,3-diphenylpropan-1-one, was synthesized and subsequently tested in an attempt to test the validity of the enone pharmocophore model, which is based on a proposed 1,4-addition within a hypothetical receptor. The clear lack of activity displayed by the saturated propanone derivative, 4.4% at 1 μg/mL, -1.8% at 3 μg/mL, 18.9% at 6 μg/mL, and 50.6% at 9 μg/mL, lends credence to the proposed necessity of the electrophilic enone moiety for biological activity. The 1,3-diphenylpropynone derivative, compound **32**, was synthesized in an effort to assess the potential biological efficacy of alkynone derivatives. While not as active as its enone counterpart chalcone, compound **32** did exhibit impressive antiproliferative activity at higher concentrations. Consequently, alkynone derivatives are currently being contemplated as future synthetic targets.

The standard enone derivatives presented in Tables 1 and 2 explored the biological effects of aromatic substitution extensively. The majority of the most active compounds contained functionalizations at the *ortho* positions of their aromatic rings. In many cases, these functional groups were electron withdrawing in nature and may have helped to isolate the enone linker from the rest of the molecule, thereby augmenting its electrophilic nature resulting in increased availability for nucleophilic attack. Electron donating substituents however did not show a reliable increase in activity when they were present in a molecule.

Tables 3 and 4 contain the napthyl, anthryl, and biphenyl enone derivatives (see Figure 8). These analogs were designed and synthesized in an effort to study the effect that increased steric bulk in the aromatic regions of the pharmocophore would have on their overall biological activity. In a direct comparison to the standard enone analogs, the multi-ring aromatic derivatives did not exhibit the same level of *in vitro* inhibition in the SVR assays. Compounds

Table 3. Total Cell Count Data from *in vitro* SVR Cell Assays of Napthyl/Anthryl/Biphenyl Enone Analogs

Compound	Total SVR Cell Count			
	1 µg/ml	**3 µg/ml**	**6 µg/ml**	**9 µg/ml**
1-Naphthalen-2-yl-3-phenylpropenone (33)	77380	13060	6980	5220
3-Naphthalen-2-yl-1-phenylpropenone (34)	283620	69120	94840	126560
1-Biphenyl-4-yl-3-phenylpropenone (35)	160120	101200	168800	----
1,3-Bis-biphenyl-4-ylpropenone (36)	144520	155920	153600	----
3-Biphenyl-4-yl-1-phenylpropenone (37)	134280	134920	83360	----
3-(2,6-Dichlorophenyl)-1-naphthalen-2-ylpropenone (38)	246260	181500	8860	4320
3-(4-Benzyloxyphenyl)-1-(4-chlorophenyl)propenone (39)	127940	135140	47700	----
3-(4-Benzyloxyphenyl)-1-p-tolylpropenone (40)	140280	134120	106820	----
1-Anthracen-9-yl-3-phenylpropenone (41)	133200	83080	44120	----
3-Anthracen-9-yl-1-phenylpropenone (42)	81200	72000	40800	----
1-Anthracen-9-yl-3-naphthalen-2-ylpropenone (43)	84880	66120	73760	----
1-Naphthalen-1-yl-3-phenylpropenone (44)	159360	103440	45440	----
1,3-Dianthracen-9-ylpropenone (45)	139900	127160	97280	----
3-Naphthalen-1-yl-1-naphthalen-2-ylpropenone (46)	107240	76620	50680	----
3-Naphthalen-2-yl-1-naphthalen-1-ylpropenone (47)	102440	79220	48960	----
1,3-Dinaphthalen-1-ylpropenone (48)	89780	45400	40560	----

33, 1-naphthalen-2-yl-3-phenylpropenone, and **38**, 3-(2,6-dichlorophenyl)-1-naphthalen-2-ylpropenone, each exhibited high levels of activity at concentrations of 3, 6, and 9 µg/mL (67.9-78.5%, 89.6-92.4% and 90.8-99.0% respectively), but did not show appreciable activity at the lower concentration of 1 µg/mL. Compounds **42**, 3-anthracen-9-yl-1-phenylpropenone, and **43**, 1-anthracen-9-yl-3-naphthalen-2-ylpropenone, show moderate activity (approximately 50%) at 3, 6, and 9 µg/mL. These four compounds are the most active of this class of enone. The activity expressed by the 2-napthyl and 9-anthryl analogs does suggest a certain amount of latitude with regards to steric bulk in the aromatic regions of the design model. As was observed with the standard enone derivatives, the 3-(2,6-dichlorophenyl)-1-naphthalen-2-ylpropenone derivative

Table 4. Percent Inhibition of *in vitro* SVR Cell Proliferation by Napthyl/Anthryl/Biphenyl Enone Analogs

Compound	SVR Percent Growth Inhibition			
	1 µg/ml	**3 µg/ml**	**6 µg/ml**	**9 µg/ml**
1-Naphthalen-2-yl-3-phenylpropenone (33)	-27.1	78.5	89.6	90.8
3-Naphthalen-2-yl-1-phenylpropenone (34)	-52.4	79.7	57.1	66.2
1-Biphenyl-4-yl-3-phenylpropenone (35)	10.4	34.7	0.0	----
1,3-Bis-biphenyl-4-ylpropenone (36)	19.2	0.0	0.0	----
3-Biphenyl-4-yl-1-phenylpropenone (37)	24.9	12.9	41.4	----
3-(2,6-Dichlorophenyl)-1-naphthalen-2-ylpropenone (38)	-43.7	67.9	92.4	99.0
3-(4-Benzyloxyphenyl)-1-(4-chlorophenyl)propenone (39)	25.6	4.4	62.9	----
3-(4-Benzyloxyphenyl)-1-p-tolylpropenone (40)	18.4	5.1	17.0	----
1-Anthracen-9-yl-3-phenylpropenone (41)	25.5	46.4	69.0	----
3-Anthracen-9-yl-1-phenylpropenone (42)	54.6	53.5	71.3	----
1-Anthracen-9-yl-3-naphthalen-2-ylpropenone (43)	52.5	57.3	48.1	----
1-Naphthalen-1-yl-3-phenylpropenone (44)	10.9	33.2	68.2	----
1,3-Dianthracen-9-ylpropenone (45)	0.0	0.0	4.7	----
3-Naphthalen-1-yl-1-naphthalen-2-ylpropenone (46)	0.0	24.9	50.3	----
3-Naphthalen-2-yl-1-naphthalen-1-ylpropenone (47)	0.0	22.4	52.0	----
1,3-Dinaphthalen-1-ylpropenone (48)	12.0	55.5	60.3	----

38, containing two chlorine substituents on its *ortho* positions, was one of the most effective compounds tested in this group.

The next collection of compounds presented are the 5-benzo[1,3]dioxole derivatives. These analogs were evaluated for three primary reasons. The first was additional investigation into steric bulk constraints in the aromatic regions of the pharmocophore. The second was an attempt to identify active compounds that possessed potentially hydrophilic functional groups for their inclusion in the mouse trials discussed in Chapter 3 of this manuscript. The third reason was an effort to reduce hydroxylation, metabolism, and other metabolic reactions. The overall results from the SVR assays for these compounds were somewhat disappointing. Only three of

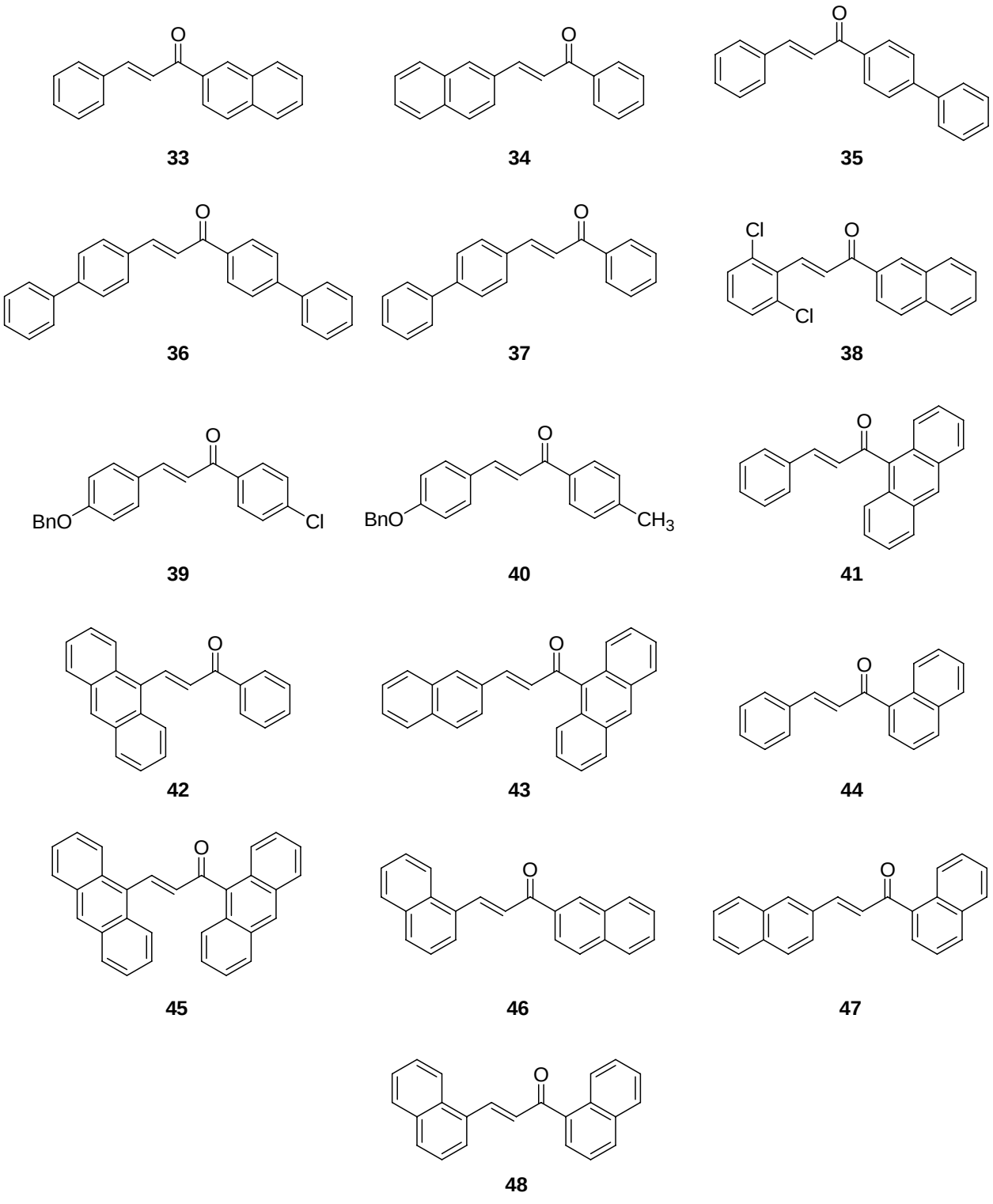

Figure 8. Structures of Compounds **33-48** from Tables 3 and 4

Table 5. Total Cell Count Data from *in vitro* SVR Cell Assays of 5-Benzo[1,3]dioxole Analogs

Compound	Total SVR Cell Count			
	1 µg/ml	3 µg/ml	6 µg/ml	9 µg/ml
3-Benzo[1,3]dioxol-5-yl-1-(3,4-dimethoxyphenyl)propenone (49)	136960	109640	75480	50500
3-Benzo[1,3]dioxol-5-yl-1-naphthalen-2-ylpropenone (50)	131680	142680	128260	88080
3-Benzo[1,3]dioxol-5-yl-1-p-tolylpropenone (51)	109980	153400	157540	142140
3-Benzo[1,3]dioxol-5-yl-1-(4-methoxyphenyl)propenone (52)	138280	123760	79320	56460
3-Benzo[1,3]dioxol-5-yl-1-(2-hydroxyphenyl)propenone (53)	121600	135800	103780	77200
3-Benzo[1,3]dioxol-5-yl-1-phenylpropenone (54)	132060	102160	26440	15340
3-Benzo[1,3]dioxol-5-yl-1-pyridin-3-ylpropenone (55)	128140	104900	42700	15380
3-Benzo[1,3]dioxol-5-yl-1-pyridin-2-ylpropenone (56)	137180	86860	29700	22560

Table 6. Percent Inhibition of *in vitro* SVR Cell Proliferation by 5-Benzo[1,3]dioxole Analogs

Compound	SVR Percent Growth Inhibition			
	1 µg/ml	3 µg/ml	6 µg/ml	9 µg/ml
3-Benzo[1,3]dioxol-5-yl-1-(3,4-dimethoxyphenyl)propenone (49)	1.9	24.2	48.1	65.6
3-Benzo[1,3]dioxol-5-yl-1-naphthalen-2-ylpropenone (50)	5.7	1.4	11.9	39.9
3-Benzo[1,3]dioxol-5-yl-1-p-tolylpropenone (51)	21.3	-6.0	-8.2	0.0
3-Benzo[1,3]dioxol-5-yl-1-(4-methoxyphenyl)propenone (52)	1.0	14.4	45.5	61.5
3-Benzo[1,3]dioxol-5-yl-1-(2-hydroxyphenyl)propenone (53)	36.5	12.7	24.5	53.4
3-Benzo[1,3]dioxol-5-yl-1-phenylpropenone (54)	31.0	34.3	80.8	90.7
3-Benzo[1,3]dioxol-5-yl-1-pyridin-3-ylpropenone (55)	33.0	32.5	68.9	90.7
3-Benzo[1,3]dioxol-5-yl-1-pyridin-2-ylpropenone (56)	28.3	44.1	78.4	86.4

the eight compounds tested showed any noteworthy activity. Compound **54**, 3-benzo[1,3]dioxol-5-yl-1-phenylpropenone, compound **55**, 3-benzo[1,3]dioxol-5-yl-1-pyridin-3-ylpropenone, and compound **56**, 3-benzo[1,3]dioxol-5-yl-1-pyridin-2-ylpropenone, exhibited 28.3-33.0% inhibition at 1 µg/mL, 32.5-44.1% inhibition at 3 µg/mL, 68.9-80.8% inhibition at 6 µg/mL, and 86.4-90.7% inhibition at 9 µg/mL. Direct comparison with their standard enone counterparts, chalcone (**1**) and the (2/3-pyridyl)phenylpropenones (**22** and **23**) shows a moderate drop in

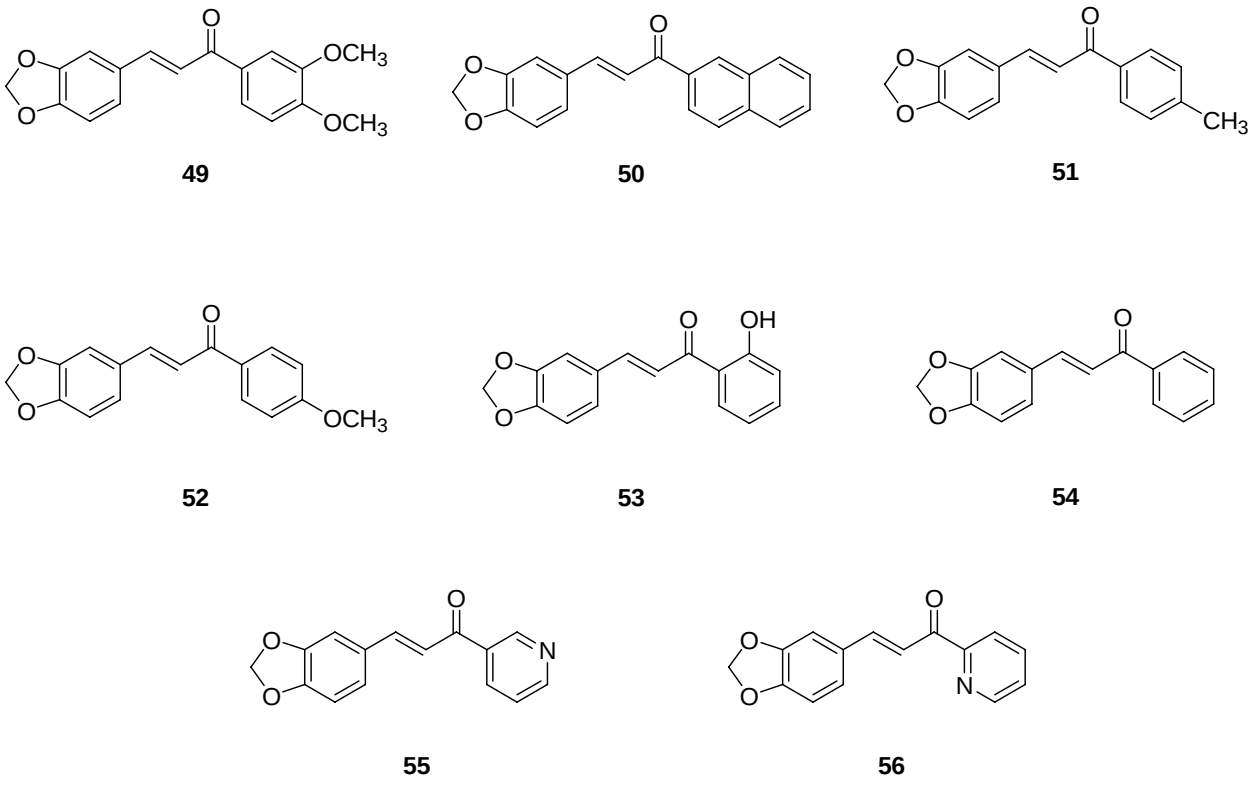

Figure 9. Structures of Compounds **49-56** from Tables 5 and 6

activity as a result of the benzo[1,3]dioxole ring addition. In addition to their average activity, the benzo[1,3]dioxole rings did not result in any appreciable increase in solubility for the analogs. As a result, these derivatives were not included in the *in vivo* trials detailed in Chapter 3.

The effects of six membered and polycyclic aromatic rings on the biological efficacy of various enone derivatives had been extensively investigated at this point. The compounds presented in Tables 7-8 and Figure 10 were designed and synthesized in an effort to explore the effect that analogs containing five membered, heterocyclic rings would have on SVR cell growth inhibition. Five compounds were prepared incorporating furyl and pyrrolyl aromatic rings.

Table 7. Total Cell Count Data from *in vitro* SVR Cell Assays of Furan/Pyrrole Analogs

Compound	Total SVR Cell Count			
	1 µg/ml	3 µg/ml	6 µg/ml	9 µg/ml
1,3-Difuran-2-ylpropenone (57)	165000	142320	125160	----
3-Furan-2-yl-1-phenylpropenone (58)	161360	153360	175120	----
1-Furan-2-yl-3-phenylpropenone (59)	73220	43140	10020	----
3-Phenyl-1-(1H-pyrrol-2-yl)propenone (60)	93540	90400	82240	----
1-Phenyl-3-(1H-pyrrol-2-yl)propenone (61)	82700	80140	101680	----

Table 8. Percent Inhibition of *in vitro* SVR Cell Proliferation by Furan/Pyrrole Analogs

Compound	SVR Percent Growth Inhibition			
	1 µg/ml	3 µg/ml	6 µg/ml	9 µg/ml
1,3-Difuran-2-ylpropenone (57)	7.7	8.1	12.0	----
3-Furan-2-yl-1-phenylpropenone (58)	9.8	1.0	0.0	----
1-Furan-2-yl-3-phenylpropenone (59)	28.2	57.7	90.2	----
3-Phenyl-1-(1H-pyrrol-2-yl)propenone (60)	8.3	11.4	19.4	----
1-Phenyl-3-(1H-pyrrol-2-yl)propenone (61)	19.0	21.5	0.4	----

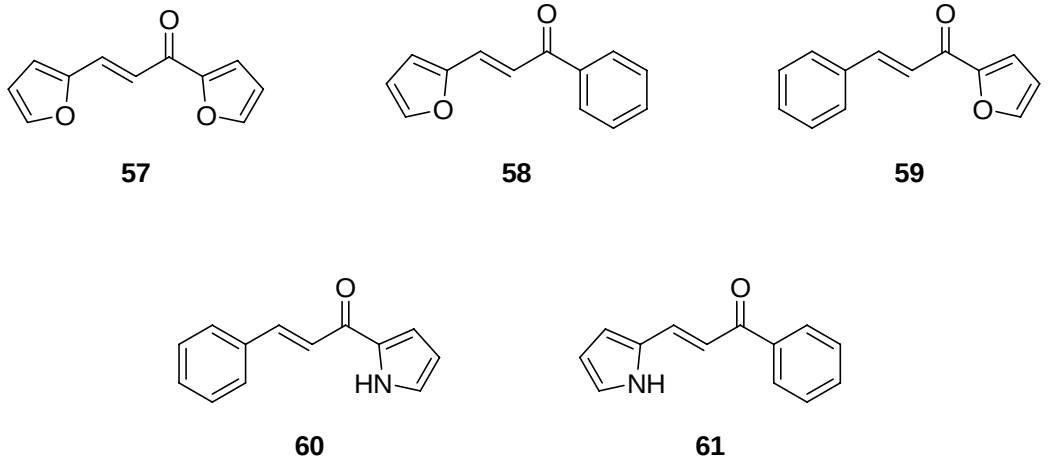

Figure 10. Structures of Compounds **57-61** from Tables 7 and 8

Compound **59**, 1-furan-2-yl-3-phenylpropenone, was the only derivative shown to inhibit SVR cell proliferation to any measurable degree. Upon direct comparison to their standard enone counterparts and curcumin itself, the furyl and pyrrolyl analogs' lack of general activity seems to verify the importance of the six membered aromatic rings found in the pharmocophore model. A mild tolerance of polycyclic aromatic moieties has been observed, but the smaller, heterocyclic furan and pyrrole rings may not have the necessary steric bulk to effectively interact with the receptor site responsible for the analogs' antiproliferative activity.

The final enone derivatives to be presented are the tetralone analogs contained in Tables 9-10 and Figure 11. The inclusion of the two methylene groups connecting the number 2 carbon of the propenone chain and the *ortho* position of the benzene ring results in a rigidification of the molecule, as well as the addition of steric bulk. The analogs were patterned after previously synthesized compounds (chalcone, napthyl, dichloro enones). Compound **63**, 2-(2,6-dichlorobenzylidene)-3,4-dihydro-2H-naphthalen-1-one, exhibited moderate antiproliferative activity, while the two napthyl derivatives demonstrated significant activity. Compound **64**, 2-naphthalen-2-ylmethylene-3,4-dihydro-2H-naphthalen-1-one, exhibited 84.6% inhibition at 1 μg/mL, 84.8% inhibition at 3 μg/mL, 80.5% inhibition at 6 μg/mL, and 79.6% inhibition at 9 μg/mL making it one of the best antiproliferative agents discovered to date. Compound **65**, showed little activity at the 1 μg/mL concentration, but performed well at higher doses (see Table 10).

During the preparation and evaluation of the aforementioned enone analogs, several dienone derivatives were synthesized as well in an effort to expand the range of potential angiogenic inhibitors under investigation and to test the validity of the dienone pharmocophore proposed in Chapter 1. The biological test results for the initial compounds were very promising

Table 9. Total Cell Count Data from *in vitro* SVR Cell Assays of Tetralone Analogs

Compound	Total SVR Cell Count			
	1 µg/ml	3 µg/ml	6 µg/ml	9 µg/ml
2-Benzylidene-3,4-dihydro-2H-naphthalen-1-one (62)	264640	248700	166220	93080
2-(2,6-Dichlorobenzylidene)-3,4-dihydro-2H-naphthalen-1-one (63)	68540	64300	47260	----
2-Naphthalen-2-ylmethylene-3,4-dihydro-2H-naphthalen-1-one (64)	9400	9240	13020	11620
2-Naphthalen-1-ylmethylene-3,4-dihydro-2H-naphthalen-1-one (65)	60760	14500	29380	12120

Table 10. Percent Inhibition of *in vitro* SVR Cell Proliferation by Tetralone Analogs

Compound	SVR Percent Growth Inhibition			
	1 µg/ml	3 µg/ml	6 µg/ml	9 µg/ml
2-Benzylidene-3,4-dihydro-2H-naphthalen-1-one (62)	0.0	27.0	24.8	75.1
2-(2,6-Dichlorobenzylidene)-3,4-dihydro-2H-naphthalen-1-one (63)	32.8	37	53.7	----
2-Naphthalen-2-ylmethylene-3,4-dihydro-2H-naphthalen-1-one (64)	84.6	84.8	80.5	79.6
2-Naphthalen-1-ylmethylene-3,4-dihydro-2H-naphthalen-1-one (65)	0.2	76.1	56.1	78.7

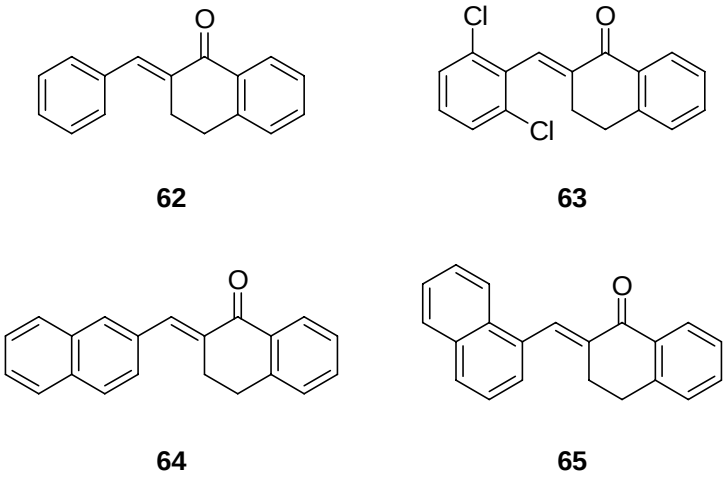

62 **63**

64 **65**

Figure 11. Structures of Compounds **62-65** from Tables 9 and 10

and the focus of the project shifted to further the study of these new derivatives. All of the dienone analogs synthesized and biologically evaluated to date are provided in Tables 11-14. They have been divided into two separate groups for ease of consideration. The first grouping contains the "acetone" dienone derivatives. They possess a pentadienone linker and a variety of aromatic moieties (see Table 11-12 and Figure 12). In general, their biological activity has been encouraging. A number of the most active compounds discovered so far originate from this particular category of dienone analogs. Compound **66,** 1,5-Diphenylpenta-1,4-dien-3-one, resulted in 86.1% inhibition at 1 μg/mL, 96.6% inhibition at 3 μg/mL, 97.7% inhibition at 6 μg/mL and 97.3% inhibition at 9 μg/mL. The two halogenated derivatives, 1,5-bis(2-chloro-6-fluorophenyl)penta-1,4-dien-3-one (**67**) and 1,5-bis(2,6-dichlorophenyl)penta-1,4-dien-3-one (**68**) also show significant antiproliferative activity over the entire range of drug concentrations. These results epitomize the similar successes attained by other *ortho* substituted analogs. Compounds **69** and **70** each contain electron donating substituents (methoxy and dimethyl amino groups), but their overall activity is higher than would have been originally anticipated given the results from similarly substituted enone analogs. Compound **75**, 1,5-bis(naphthalen-1-yl)penta-1,4-dien-3-one, also shows noteworthy activity at the higher doses of 6 and 9 μg/mL. The additional napthyl and anthryl pentdienone analogs do not show any appreciable activity however. Perhaps the expanded linker region of the dienone pharmacophore has a negative impact on the receptor site's steric tolerance of multi-cyclic aromatic moeities. As was to be expected, based on the chalcone analog results, the furyl and benzo[1,3]dioxole containing analogs showed marginal, if any, biological efficacy.

The second category of dienone derivatives investigated contain a 2,6-dimethylenecyclohexanone core (see Tables 13-14 and Figure 13). These analogs bear some

Table 11: Total Cell Count Data from *in vitro* SVR Cell Assays of Dienone-Acetone Analogs

Compound	Total SVR Cell Count			
	1 µg/ml	**3 µg/ml**	**6 µg/ml**	**9 µg/ml**
1,5-Diphenylpenta-1,4-dien-3-one (66)	46280	8880	6160	7280
1,5-Bis(2-chloro-6-fluorophenyl)penta-1,4-dien-3-one (67)	76800	45480	19080	----
1,5-Bis(2,6-dichlorophenyl)penta-1,4-dien-3-one (68)	70200	19920	13600	----
1,5-Bis(2,6-dimethoxyphenyl)penta-1,4-dien-3-one (69)	20960	6520	5020	4840
1,5-Bis(4-dimethylaminophenyl)penta-1,4-dien-3-one (70)	1067400	949920	821400	627400
1,5-Difuran-2-ylpenta-1,4-dien-3-one (71)	129740	92580	44380	----
1,5-Bisbenzo[1,3]dioxol-5-ylpenta-1,4-dien-3-one (72)	158920	126720	120700	103780
1-Benzo[1,3]dioxol-5-yl-5-phenylpenta-1,4-dien-3-one (73)	150240	126760	60300	6080
1,5-Bis(naphthalen-2-yl)penta-1,4-dien-3-one (74)	33620	32920	29480	28100
1,5-Bis(naphthalen-1-yl)penta-1,4-dien-3-one (75)	33740	22520	4460	4140
1,5-Bis(anthracen-9-yl)penta-1,4-dien-3-one (76)	27740	28980	29120	23840

Table 12: Percent Inhibition of *in vitro* SVR Cell Proliferation by Dienone-Acetone Analogs

Compound	SVR Percent Growth Inhibition			
	1 µg/ml	**3 µg/ml**	**6 µg/ml**	**9 µg/ml**
1,5-Diphenylpenta-1,4-dien-3-one (66)	86.1	96.6	97.7	97.3
1,5-Bis(2-chloro-6-fluorophenyl)penta-1,4-dien-3-one (67)	57.0	70.6	86.6	----
1,5-Bis(2,6-dichlorophenyl)penta-1,4-dien-3-one (68)	60.7	87.1	90.4	----
1,5-Bis(2,6-dimethoxyphenyl)penta-1,4-dien-3-one (69)	33.8	77.8	79.7	82.7
1,5-Bis(4-dimethylaminophenyl)penta-1,4-dien-3-one (70)	34.0	41.3	49.2	61.2
1,5-Difuran-2-ylpenta-1,4-dien-3-one (71)	0.0	9.3	56.5	----
1,5-Bisbenzo[1,3]dioxol-5-ylpenta-1,4-dien-3-one (72)	-13.8	12.4	17.1	29.2
1-Benzo[1,3]dioxol-5-yl-5-phenylpenta-1,4-dien-3-one (73)	21.5	18.5	56.1	96.3
1,5-Bis(naphthalen-2-yl)penta-1,4-dien-3-one (74)	-6.3	-12.0	-19.1	-0.4
1,5-Bis(naphthalen-1-yl)penta-1,4-dien-3-one (75)	-6.6	23.3	82.0	85.2
1,5-Bis(anthracen-9-yl)penta-1,4-dien-3-one (76)	12.3	1.4	-17.6	14.9

resemblance to the tetralone enone derivatives previously described. While not as rigid as their tetralone counterparts, the dimethylenecyclohexanone derivatives do contain increased steric bulk as a result of the three additional methylene groups present on the central linker. The two most active cyclohexanone dienone derivatives are compounds **81** and **83**. Each contains two

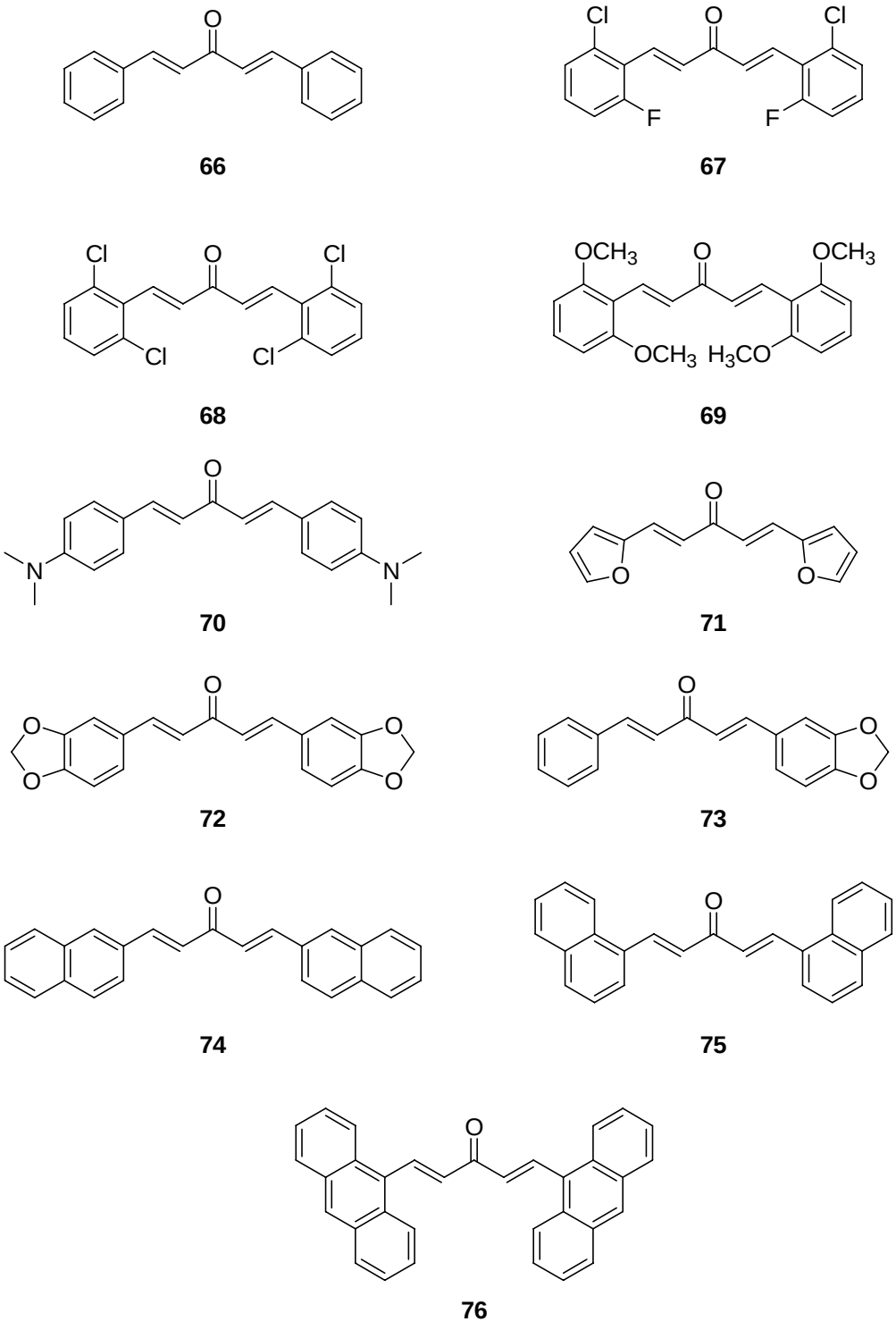

Figure 12: Structure of Compounds 66-76 from Tables 11 and 12

pyridyl rings in place of the substituted benzene moieties found in the general dienone pharmocophore. These compounds were investigated after the biological results from the corresponding pyridyl enone analogs showed significant activity. Coumpound **81**, 2,6-di(pyridin-2-ylmethylene)cyclohexanone, was shown to inhibit SVR cell proliferation by 57.4% at 1 μg/mL, 92.7% at 3 μg/mL, 94.3% at 6 μg/mL and 96.5% at 9 μg/mL. Even more impressive were the results for the 4-pyridyl analog, 2,6-di(pyridin-4-ylmethylene)cyclohexanone (**83**), which inhibited cell proliferation by 86.5, 90.0, 95.5 and 98.4% for the 1, 3, 6 and 9 μg/mL concentrations. As a direct result of these impressive levels of biological efficacy, a mixed 2-pyridyl/phenyl derivative (**82**) was examined. While not as active as its dipyridyl counterparts, it did however, show moderate activity at low to mid concentrations and significant activity at the highest concentration of 9 μg/mL. In addition to the pyridyl analogs, the prototypical cyclohexanone derivative, 2,6-dibenzylidenecyclohexanone (**78**) registered significant antiproliferative activity. It was shown to inhibit SVR cell growth by 49.9% at 1 μg/mL, 94.4% at 3 μg/mL, 97.7% at 6 μg/mL, and 97.6% at 9 μg/mL. Rounding out the most active analogs of this particular category of dienone derivatives was compound **84**, 2,6-di(4-hydroxy-3-methoxybenzylidene)cyclohexanone. This particular analog is perhaps the closest approximation of curcumin evaluated to date. The substitution patterns of its aromatic moieties are identical to those of curcumin, and the dienone linker provides a close approximation of the β-diketone region found in the original parent compound. The compound's activity is on par with the dipyridyl analogs. It exhibits 61.4% inhibition at 1 μg/mL, 90.1% at 3 μg/mL, 96.0% at 6 μg/mL, and 97.7% at 9 μg/mL. A pentadienone version of this compound is a logical target for future synthetic efforts. Even with all its success, this group of dienone analogs did contain several poor to inactive compounds. Uncharacteristically, the *ortho* substituted cyclohexanone

Table 13: Total Cell Count Data from *in vitro* SVR Cell Assays of Dienone-Cycloalkanone Analogs

Compound	Total SVR Cell Count			
	1 µg/ml	3 µg/ml	6 µg/ml	9 µg/ml
2,5-Dibenzylidenecyclopentanone (77)	138240	107780	79000	----
2,6-Dibenzylidenecyclohexanone (78)	167080	14680	6160	6560
2,6-Bis(2,6-dichlorobenzylidene)cyclohexanone (79)	93460	71600	74360	----
2,6-Di(2-chloro-6-fluorobenzylidene)cyclohexanone (80)	289340	182820	103720	42760
2,6-Di(pyridin-2-ylmethylene)cyclohexanone (81)	142000	19080	15280	9480
2-Benzylidene-6-pyridin-2-ylmethylenecyclohexanone (82)	1104320	871080	539840	70720
2,6-Di(pyridin-4-ylmethylene)cyclohexanone (83)	45080	26120	12240	4360
2,6-Di(4-hydroxy-3-methoxybenzylidene)cyclohexanone (84)	607520	156520	63480	36120
2,6-Di(naphthalen-1-ylmethylene)cyclohexanone (85)	85860	96700	90440	----
2,6-Di(naphthalen-2-ylmethylene)cyclohexanone (86)	86760	75820	86480	----
2,6-Di(anthracen-9-ylmethylene)cyclohexanone (87)	27680	22000	30340	38340
3,5-Di(4-hydroxy-3-methoxybenzylidene)tetrahydropyran-4-one (88)	788840	642000	60520	68120

Table 14: Percent Inhibition of *in vitro* SVR Cell Proliferation by Dienone-Cycloalkanone Analogs

Compound	SVR Percent Growth Inhibition			
	1 µg/ml	3 µg/ml	6 µg/ml	9 µg/ml
2,5-Dibenzylidenecyclopentanone (77)	19.6	23.8	38.6	----
2,6-Dibenzylidenecyclohexanone (78)	49.9	94.4	97.7	97.6
2,6-Bis(2,6-dichlorobenzylidene)cyclohexanone (79)	8.4	29.8	27.1	----
2,6-Di(2-chloro-6-fluorobenzylidene)cyclohexanone (80)	2.2	40.3	64.4	85.7
2,6-Di(pyridin-2-ylmethylene)cyclohexanone (81)	57.4	92.7	94.3	96.5
2-Benzylidene-6-pyridin-2-ylmethylenecyclohexanone (82)	24.5	39.2	59.6	95.0
2,6-Di(pyridin-4-ylmethylene)cyclohexanone (83)	86.5	90.0	95.5	98.4
2,6-Di(4-hydroxy-3-methoxybenzylidene)cyclohexanone (84)	61.4	90.1	96.0	97.7
2,6-Di(naphthalen-1-ylmethylene)cyclohexanone (85)	15.9	5.2	11.4	----
2,6-Di(naphthalen-2-ylmethylene)cyclohexanone (86)	15.0	25.7	15.2	----
2,6-Di(anthracen-9-ylmethylene)cyclohexanone (87)	12.5	25.1	-22.5	-36.9
3,5-Di(4-hydroxy-3-methoxybenzylidene)tetrahydropyran-4-one (88)	51.2	60.3	96.3	95.8

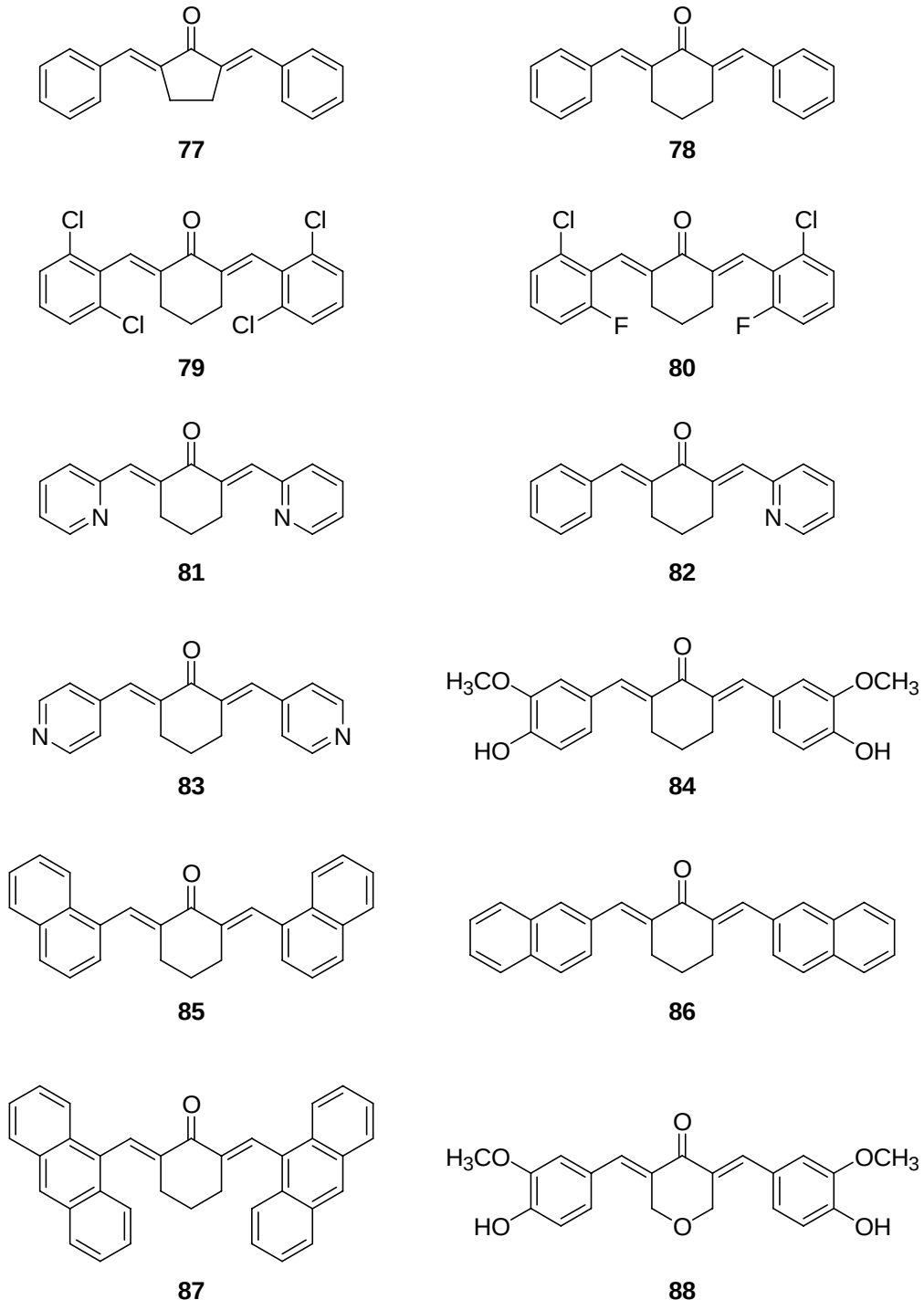

Figure 13: Structures of Compounds 77-88 from Tables 13 and 14

analogs did not show very impressive levels of activity in comparison with their enone and pentadienone counterparts. The napthyl and anthryl derivatives exhibited even less activity. Overall, however, this group of dienone analogs contains some of the most intriguing compounds evaluated during the course of the study.

At this point in the project's ongoing development, a significant number of the novel curcumin derivatives had been shown to exhibit high levels of *in vitro* activity in the SVR endothelial cell assays. Many of the top enone and dienone analogs exhibited over 90% inhibition at numerous concentrations. The question that naturally arose from these results was how these compounds were to be assessed in relation to one another. Which analogs were to be considered the most active when each exhibited roughly the same level of activity? For the top five derivatives of both the enone and dienone subcategories, each was shown to exhibit high levels of efficacy at the current concentrations used in the antiproliferation assays (1, 3, 6 and 9 μg/mL). The next logical step in the evolution of the project was determined to be a dose-response study of the most active analogs identified to date. For the pilot study, however, the choice of compounds to be investigated was not based solely on biological activity. Structural variability was also factored into the selection process in an effort to obtain detailed low dose activity data on a wide variety of structurally diverse derivatives. The enone analogs chosen for inclusion in the study are identified in Table 15. The drug concentrations used for the trials were 3.0, 1.0, 0.3, 0.1, and 0.03 μg/mL. These concentrations were chosen so that an inverse log plot of the reported activities could be generated in an attempt to determine the EC_{50} dose for each of the compounds. The experimental conditions and procedures for these assays remained the same as previously described. Only the compound concentrations were varied. Tables 15 and 16 detail the results from the first trial attempted for the enone derivatives. Tables 17 and 18

contain the data obtained from the second enone dose response trial. The dienone analogs included in these studies and their subsequent activities are provided in Tables 19 and 20.

Upon examining the data generated from these studies, it became fairly obvious that some aspect of the dose response assays had gone awry. The 1 and 3 μg/mL concentrations were included in the studies as a means of validating the results. Ideally, the data generated in these trials at those particular concentrations should have correlated with the original data presented earlier in the document (Tables 1-14). This was not found to be the case. In numerous instances the dose response data differed significantly from the previously recorded values, calling into question the validity of these particular studies. As an example, Chalcone showed a marked deviation from its former levels of activity. Many of the compounds show a loss of all activity at one concentration followed by a steep resurgence at a lower concentration. Variations within the control well cell counts were also cause for concern. A difference of 10 – 20 thousand cells was observed between the second enone assay and the initial dienone study. These assays were performed on the same day using identically prepared cell culture plates. Regardless of the initial results of the dose response studies, they still represent an important part of future curcumin derivative research. Additional trials should be performed in an effort to determine where the current difficulties lie. Obtaining accurate EC_{50} values for the top performing derivatives will aid in the development of increasingly active compounds in the future.

Compounds 1-13, 15-27, 29-31, 33-48, 57-68, 71, 77-79, 81, 85, and 86 have been previously reported in the dissertation of Dr. Phillip Robinson, who was responsible for their synthesis and evaluation. Compounds 14, 28, 32, 49-56, 69, 70, 72-76, 80, 82-84, 87, and 88 were tested by Mr. Richard Hubbard. Of those compounds, 14, 28, 49-56, 70, 72, 73, 84, and 88 were obtained from commercial sources for their inclusion in these studies. All additional

compounds were synthesized in the Bowen laboratory. The full spectrum of enone and dienone data is included herein to provide the reader with a complete overview concerning the Bowen laboratory's work in this area.

Table 15. Total SVR Cell Count Data from the Initial Enone Dose Response Study

Compound	SVR Total Cell Count				
	3 µg/ml	**1 µg/ml**	**0.3 µg/ml**	**0.1 µg/ml**	**0.03 µg/ml**
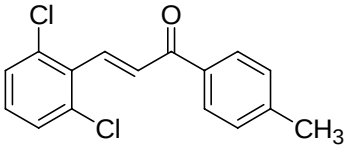	4207	7347	9845	7115	5964
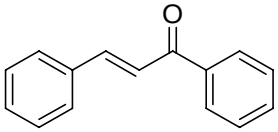	7043	7405	7055	5862	6307
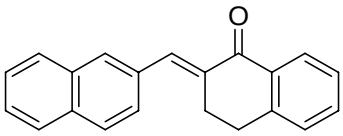	1215	2506	5738	8116	8526
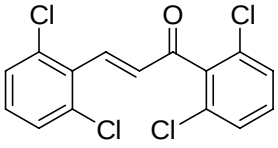	899	5204	6008	8381	5577
Control	7997	6318	10556	7073	----

Table 16. Percent SVR Cell Growth Inhibition from the Initial Enone Dose Response Study

Compound	SVR Percent Inhibition				
	3 µg/ml	**1 µg/ml**	**0.3 µg/ml**	**0.1 µg/ml**	**0.03 µg/ml**
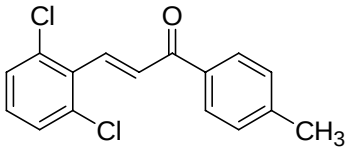	47.3	8	-23.3	10.9	25.3
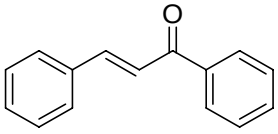	11.8	7.3	11.7	26.6	21
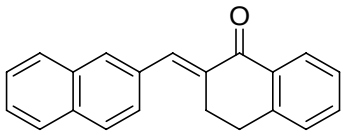	84.8	68.6	28.1	-1.6	-6.8
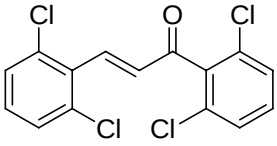	88.7	34.8	24.8	-4.9	30.2

Table 17. Total SVR Cell Count Data from the Second Enone Dose Response Study

Compound	SVR Total Cell Count				
	3 µg/ml	**1 µg/ml**	**0.3 µg/ml**	**0.1 µg/ml**	**0.03 µg/ml**
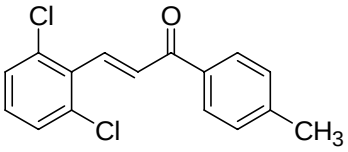	14919	17708	10798	13850	19627
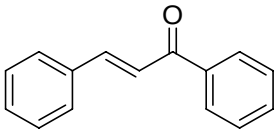	11641	13576	9937	13226	16950
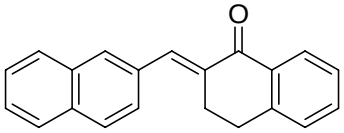	5729	8630	12308	9460	12148
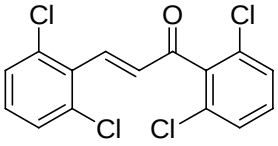	10818	11175	16863	15798	12176
Control	16170	19478	10104	19536	----

Table 18. Percent SVR Cell Growth Inhibition from the Second Enone Dose Response Study

Compound	SVR Percent Inhibition				
	3 µg/ml	**1 µg/ml**	**0.3 µg/ml**	**0.1 µg/ml**	**0.03 µg/ml**
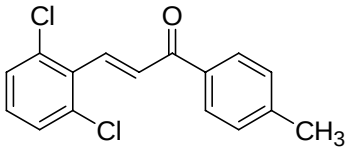	8.6	-8.5	33.8	15.1	-20.2
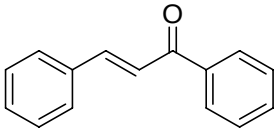	28.7	16.8	39.1	19	-3.8
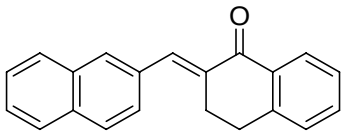	64.9	47.1	24.6	42	25.6
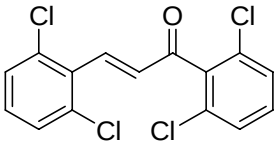	33.7	31.5	-3.3	3.2	25.4

Table 19. Total SVR Cell Count Data from the Initial Dienone Dose Response Study

Compound	Total SVR Cell Count				
	3 µg/ml	**1 µg/ml**	**0.3 µg/ml**	**0.1 µg/ml**	**0.03 µg/ml**
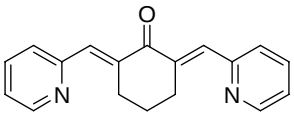	3104	6503	17690	16797	15089
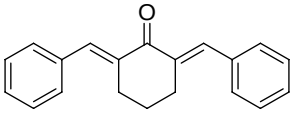	8693	18647	17929	10766	17418
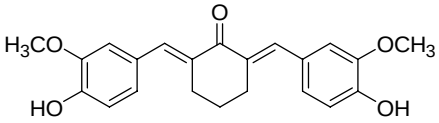	11309	13835	12742	18738	19881
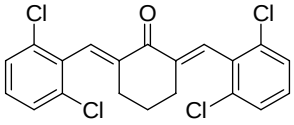	4691	5394	10415	17891	20165
Control	307200	357600	353580	338200	----

Table 20. Percent SVR Cell Growth Inhibition from the Initial Dienone Dose Response Study

Compound	Total SVR Cell Count				
	3 µg/ml	**1 µg/ml**	**0.3 µg/ml**	**0.1 µg/ml**	**0.03 µg/ml**
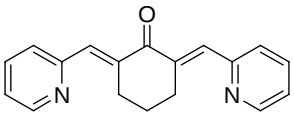	81.7	61.7	-4.3	0.9	11
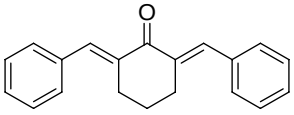	48.7	-10	-5.7	36.5	-2.7
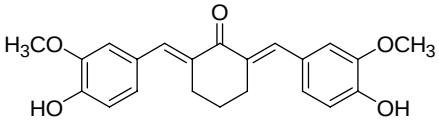	33.3	18.4	24.9	-10.5	-17.2
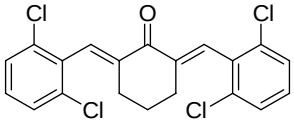	72.3	68.2	38.6	-5.5	-18.9

CHAPTER 3

PRELIMINARY MOUSE STUDIES

Overview and Experimental Design

In vivo mouse studies of the aromatic enone and dienone curcumin analogs discussed in the preceding chapters were undertaken in late 2002/early 2003 as a collaborative effort between the University of Georgia's College of Veterinary Medicine, Department of Chemistry, and Emory University School of Medicine. The principal investigators were Dr. Nicole Northrup, DVM, DACVIM (oncology) and Dr. Phillip Bowen, PhD (medicinal chemistry). Drs Karen Cornell, DVM, DACVS, PhD and Nancy Steadman, DVM, PhD were also connected to the collaboration as co-invesigators for the College of Veternary Medicine. The overall goal of the project was the development and *in vivo* evaluation of novel antiangiogenic agents for the eventual treatment of both veterinary and human cancer patients. The curcumin derivatives that demonstrated biological efficacy and low toxicity in the murine models utilized in the study were intended to progress to clinical trials in canine oncology patients. The successful treatment of canine oncology patients would then open up the possibly of attempting phase I human trials in collaboration with Dr. Jack Arbiser, MD, PhD (dermatology) at Emory University in Atlanta, GA.

The curcumin derivatives chosen for inclusion in these mouse trials were evaluated using murine models of two specific types of canine neoplasia. These were identified as canine osteosarcoma and prostatic carcinoma. Spontaneous osteosarcoma and prostatic carcinoma found in canines have been shown to function as naturally occurring models of these same

cancers in humans.[29,30] As such, they were judged ideal for the task at hand. These cancer types are known both to be locally aggressive and widely metastatic in canines and current treatment options are largely ineffective at halting tumor progression.[29] The typical survival time for canines diagnosed with prostatic carcinoma is approximately one month. Dogs diagnosed with osteosarcoma and treated aggressively with surgery and cytotoxic agents can survive up to one year, but only 10-30% are able to survive for up to two years.[30,31,32] The necessity for the development of new and effective means of treating these aggressive forms of cancer in both canines and humans provided the basis for the collaboration.

As previously mentioned, two different cancer types, and hence two specific cancer cell lines, were obtained for use in the *in vivo* studies performed at the UGA College of Veterinary Medicine. The canine prostate cancer cell line GN-4 was developed by Dr. David Waters at Purdue University from the lung metastasis of a dog diagnosed with spontaneous prostate cancer. Dr. Waters graciously provided the College of Veterinary Medicine with the cell samples used for this study. The GN-4 cell line is immortalized and has shown itself to be aneuploid, cytokeratin and vimentin positive and is known to form tumors in a predictable fashion when introduced subcutaneously in mice. This cell line is also known to predictably metastasize to regional lymph nodes and lung tissue. The second cell line included in the study, COS31 (canine osteosarcoma), was established by Dr. Kevin Hahn and cell samples were provided by the University of Tennessee. As with the GN-4 cell line, the COS31 cells are known to reliably produce tumors following subcutaneous injection in mice. The tumors are osteocalcin and alkaline phosphatase positive. They also produce osteoid osteoma, grow rapidly and metastasize aggressively throughout the body.[33] Utilizing cancers that are known to grow quickly and

actively metastasize, the curcumin derivatives' biological efficacy for limiting both primary and remote tumor growth can be properly evaluated.

The animals used in the study were five to six week old, male BALB/c-*nu*/*nu* (athymic) mice purchased from Harlan Sprague-Dawley. Athymic mice lack the thymus gland and consequently do not produce T cells (regulatory or cytotoxic), specific types of lymphocytes that are instrumental in controlling the body's immune response. They are involved in the eradication of both infection and any foreign matter deemed potentially harmful to the body (ie. cancer). Nude, BALB mice are commonly used in cancer research because they are predictably more tolerant to tumors and other implanted cells. The initial experimental outline called for 120 mice to be used during the course of the study. The mice were housed three to a cage. This equated to one representative from each planned treatment group per cage. The three treatment groups were defined as follows: 1) curcumin derivative one plus vehicle, 2) curcumin derivative two plus vehicle and 3) delivery vehicle alone. The specific derivatives included in the study are identified in a following section in addition to a brief explanation of how these selections were made. The animal cages were kept in microisolaters located within the rodent isolation facilities of the UGA College of Veterinary Medicine. Each cage was fitted with a High-Efficiency Particulate Air (HEPA) filter to ensure air quality. Both the water and bedding material provided for the animals were autoclaved prior to their use in order to ensure a sterile environment. The mice were fed a commercial pelleted diet and water *ad libitum*. The handling of all animals was performed in a NuAire model NU-602-400 animal cage changing, biological safety cabinet. The apparatus was monitored periodically for pathogens and any other potentially harmful particulate matter.

Prior to the onset of the animal trials, four mice were randomly assigned one of the two cancer types to be injected with and the tumors were allowed to develop in an effort to verify that the test subjects would in fact develop suitable tumors for use in the study. One million canine GN-4 prostatic carcinoma cells or COS31 canine osteosarcoma cells suspended in 0.1 mL of 0.9% NaCl saline were introduced subcutaneously into the right lateral thorax (flank) of each mouse. The mice were then monitored over the course of ten days to evaluate the size and general growth patterns of the tumors. Regrettably, a problem was encountered during this phase of the study. While the canine prostatic carcinomas were able to be replicated in the athymic mice, the canine osteosarcoma cell line was not shown to generate reliable tumors in the test animals. For this reason, it was decided that the COS31 cell line would be excluded from the animal trials, and only one tumor type would be utilized to evaluate the antiangiogenic effect of the two curcumin derivatives. All of the mice involved in the study were now to be injected with the GN-4 cell line exclusively and then randomly assigned to one of the three treatment groups previously described. All additional experimental conditions and parameters remained unaffected however. The body weight of each mouse was recorded prior to tumor cell injection and then monitored, along with tumor dimensions, twice weekly during the course of the study. The total tumor volume was calculated using the formula: $(length * width * height)\pi/6$. After the initial ten day tumor development period, the mice were to be inoculated with the appropriate curcumin derivative at a concentration of 1,500 mg/kg (diluted in 0.1 mL of 0.9% NaCl) or an equal volume of 0.9% saline alone via intraperitoneal (IP) injection. The injections were to be administered every 48 hours over the course of 20 days. On day 30 of the trial, the mice were weighed a final time and then humanely euthanized via CO_2 asphyxiation.

During the postmortem examination of the test animals, the primary tumor, lungs, and tissue samples of the area immediately surrounding the drug injection sites were collected. Each lung was divided anteriorly to posteriorly into five individual sections in preparation for a detailed analysis of tumor metastases. Each section was independently evaluated for the number and overall volume of tumor metastases present in addition to the total lung area examined. The pervasiveness of the disease was calculated as the volume of observed lung metastases divided by the total lung area inspected. Additional samples were collected from the liver, heart, kidneys, renal lymph nodes, tongue, salivary glands, spleen, intestine, pancreas, brain, stomach, trachea, seminal vesicles, prostate, coagulating gland, skeletal muscle, and skin of each test animal in an effort to detect any signs of apparent toxicity related to the administered compounds. The tissue samples were all fixed in a 10% neutral buffered formalin solution, sectioned at 5 μm, paraffin-embedded and stained with hematoxylin and eosin (H&E) in preparation for histopathologic analysis. The primary tumor itself was sectioned and mounted on charged ProbeOn™ Plus slides from Fisher Scientific after having been subjected to the same staining and embedding procedure described above. Antigen Retrieval Citra (Biogenix Laboratories Inc.), a commercially available solution, was used as part of a heat based antigen unmasking technique that was employed prior to the immunohistochemical staining of the formalin-fixed, paraffin-embedded (FFPE) tumor tissue samples. The tumor samples were deparaffinized, rehydrated with PBS, submerged in the retrieval solution (pH 6.0), and heated to near the boiling point of water using a microwave.[34,35] After twenty minutes (time is variable depending on the fixation protocol utilized), the slides were removed and stained with a primary anti-mouse CD-31 antibody from Pharmingen that selects for the endothelial cell marker CD-31. The slides were then additionally stained using a biotinylated mouse anti-rat secondary antibody

obtained from Vector Laboratories and ExtrAvidin, a strepavidin-biotin detection system from Sigma-Aldrich. The final treatment applied to the tumor sections was Gill's hematoxylin counterstain (blue), used in an effort to obtain sharp nucleus staining while minimizing any conflicting background color.

The immunohistochemistry for the study was performed using a Techmate 500 micrscope from Biotek Solutions. Healthy canine lung tissue was used as a positive control during the microvessel density evaluation of the primary tumor. The stained slides were examined manually at 400X magnification in an attempt to identify the three main areas of microvessel density. The exact number of vessels per unit area was obtained by applying a Media Cybernetics image analysis software package (Image pro Plus for Windows) to digital images taken of the magnified tumor sections. The average microvascular densities for the tumors found in each test animal are provided in Tables 22-25. These tables detail the results from the preliminary mouse studies that were undertaken in early 2003. An explanation of their significance will be provided in the Experimental Results section of this chapter. With the experimental protocols now outlined, the specific curcumin derivatives used during the course of the study will be identified along with a brief explanation as to the reasons these specific analogs were chosen for inclusion in the trials.

The compounds originally selected for use in the *in vivo* studies were 3-(2,6-Dichlorophenyl)-1-p-tolylpropenone (**3**) and 2,6-di(pyridin-2-ylmethylene)cyclohexanone (**81**). As demonstrated by the data provided in Tables 2 and 14 located in Chapter 2, these two compounds represented the most promising antiangiogenic curcumin analogs synthesized and biologically evaluated at the time of the study. The 2′,6′-dichloro-1-*p*-toluene enone analog (**3**) inhibited *in vitro* SVR endothelial cell proliferation by 73.7, 98.2, and 98.1 percent and the bis-2-

pyridylmethylenecyclohexanone analog resulted in equally impressive growth inhibition percentages of 57.4, 92.7, and 94.3. These numbers represent cell growth inhibition at the 1, 3, and 6 μg/mL concentrations. The inclusion of these particular compounds was also influenced by the fact that each one individually represented the best of the two classes of enone and dienone analogs currently under investigation. Unfortunately, after determining the quantity of compounds **3** and **81** readily available in the laboratory, it was discovered that there was an insufficient supply of these compounds for their inclusion in the animal trials. The time and material cost necessary to either synthesize additional quantities of the derivatives or purchase them from a commercial source was deemed to be prohibitive to the timely completion of the study. Each compound was, in fact, available from the Sigma-Aldrich library of rare chemicals catalog (SALOR), but the cost per 250 mg sample was roughly $50 and the quantities necessary for the study to progress were determined to be on a multigram scale. Alternative derivatives were investigated only after all means of economically acquiring the original two analogs were exhausted. The new evaluation criteria now included both the biological efficacy of the compounds in the SVR anti-proliferation assays and the ease with which multigram quantities could be synthesized and/or obtained commercially. With these qualifications in mind, the next logical choices for inclusion in the animal trials were the dienone derivatives 1,5-Diphenylpenta-1,4-dien-3-one (**66**) and 2,6-Dibenzylidenecyclohexanone (**78**). Table 11 shows that compound **66** achieved 86.1, 96.6, 97.7, and 97.3 percent SVR cell growth inhibition for the drug concentrations 1, 3, 6, and 9 μg/mL. Compound **78** achieved 49.9, 94.4, 97.7, and 97.6 percent inhibition at those same concentrations. Both derivatives were found to be available from the standard Sigma-Aldrich catalog. Compound **66** was approximately $83 per 50 g sample and compound **78** was similarly inexpensive, $133 for an equivalent amount. This satisfied both the

Table 21. Solubility Results for Compounds 66 and 78

Compound	Solvent System	Solubilty Results
1,5-Diphenylpenta-1,4-dien-3-one (66)	0.9% NaCl solution	Insoluble
	5% Dextrose	Insoluble
	95% Ethanol	100 mg / 7.0 mL
	Dimethyl Sulfoxide (DMSO)	100 mg / 0.3 mL
2,6-Dibenzylidenecyclohexanone (78)	0.9% NaCl solution	Insoluble
	5% Dextrose	Insoluble
	95% Ethanol	100 mg / 23 mL
	Dimethyl Sulfoxide (DMSO)	100 mg / 1.75 mL

time and funding constraints, while also alleviating the need for lengthy purification following a typical laboratory synthesis. In reality, compound **66** actually scored higher than either of the original analogs considered, but its hydrophobic nature initially led researchers to choose the potentially more hydrophilic heteroatom containing derivatives. The hydrophobic nature of the new compounds was evaluated through a series of solubility tests performed for a variety of proposed delivery vehicles (100 mg per solution). Table 21 details the solubility results for the two compounds. Each of the derivatives was found to be insoluble in the 0.9% NaCl saline solution originally designated for the IP drug injections. This result was not unexpected given the general structure of the analogs. A 5% dextrose saline solution was found to be equally ineffective at dissolving the compounds. This solution was originally suggested for consideration by Dr. Northrup due to the fact that it is a commonly used delivery vehicle in the treatment of canine oncology patients at the university veterinary school. Moderate success was achieved with 95% ethanol. However, the drug concentration needed for the studies was too large for such a small volume (0.1 mL) of alcohol to dissolve a sufficient amount of either

compound so that it could be injected in the manner originally suggested. The test animals would have to be exposed to enormous quantities of pure ethanol in order to deliver the appropriate concentration of the two derivatives. In addition to limited solubility, concentrated ethanol injections had been shown to result in serious skin and organ irritation in the test animals. The last solvent investigated was dimethoxy sulfoxide (DMSO). Predictably, the compounds were exceedingly soluble in DMSO. This had been demonstrated previously, as DMSO was the primary solvent system used for the anti-proliferative assays performed in the Arbiser laboratory at Emory University School of Medicine. Similar to ethanol, however, direct, undiluted injection of DMSO resulted in profound irritation of both the skin and internal organs of the test animals. Eventually the issue of finding an effective inoculation vehicle had to be resolved by fundamentally altering the method of drug administration. The use of an intraperitoneal or intravenous injection was abandoned and less invasive alternatives were considered.

The first alternative to be investigated was the oral administration of the compounds via the pelleted food used to sustain the test subjects. This idea was summarily rejected due to the potential ineffectiveness of diet mediated drug delivery. It was not possible to ensure that all of the food (and drug) provided for each mouse would be ingested. Additionally, the mice would have required isolation during feeding to ensure that no overdosing occurred due to the ingestion of a larger quantity of pellets than was allotted per subject. Feeding habits and preferences differ empirically between subjects; therefore this form of drug delivery was not utilized. The solution to this dilemma was solved with the discovery of the emulsifying agent Cremophor EL (CrEL) (polyoxyethylene glycerol triricinoleate 35). Cremophor EL is a derivative of castor oil and elthylene oxide and is commonly used as a co-solvent and emulsifying agent for both injected

and oral drug delivery. It is traditionally administered as a mixture with saline or low molecular weight alcohols. The agent formed clear solutions in water and was exceptionally soluble in ethanol. The use of Cremophor EL allowed the formation of homogenous suspensions of each derivative that could then be administered via gavage to each of the test animals. Gavage is a method of delivering a substance directly into a subject's stomach cavity through a cannula inserted down the throat. In the *in vivo* studies, a sterilized glass syringe fitted with a blunted needle tip was used to gavage the test animals. This technique required an easily digestable medium that would not act as an irritant to the subject's gastrointestinal tract. Cremophor EL satisfied both of these requirements. The use of this technique also ensured the complete delivery of the prepared drug solutions. For the purposes of this study, the drug solutions were prepared as a mixture of 2.7 mL Cremophor EL, 0.3 mL 95% ethanol (for sterilization purposes), and 300 mg of the test compounds. This produced drug solution concentrations of 100 mg/mL for both curcumin derivatives. The resulting solutions (suspensions) were initially mixed using only a magnetic stir bar (sterilized), but eventually this method was augmented with sonication. Sonication not only effectively generated a more visibly homegenous solution, but it also served as an effective means of breaking apart any aggregates formed by the compounds during the initial mixing process. With the delivery vehicle for the curcumin derivatives determined the *in vivo* studies were able to progress. The following section details the initial results generated from the studies.

Experimental Results

As was previously stated, the dose administered to each test animal was set at 1,500 mg/kg. The 5-6 week old BALB/c-*nu*/*nu* mice had an average weight of 20 g. This corresponded to roughly 30 mg of drug required per test subject. The correct gavage volume

was therefore determined to be 0.3 mL of the appropriate 100 mg/mL drug solution. This volume of vehicle was to be administered once every 48 hours over the course of 20 days as per the experimental outline. As with the initial testing of the COS31 and GN-4 cancer cell lines, the drug delivery methods and materials were subjected to a preliminary four mouse test to help ensure their viability. No control group was used for this particular study. The trial was performed using two mice per week over the course of two weeks in mid February 2003. In the initial test group, two mice were injected with the GN-4 cancer cells (prostatic carcinoma) and the resulting tumors were allowed to mature for 10 days. On the eleventh day, each mouse was randomly assigned a compound treatment solution and 0.3 mL was delivered via gavage. Unfortunately, some difficulties were encountered at this stage of the trial. The drug particles present in each suspension occasionally caused the cannula to become clogged during drug administration. This generated a certain amount of concern over the researcher's ability to accurately control the doses delivered to the mice using these suspensions. Three decisions were made as a result of this observation: 1) the compounds were to be ground as fine as possible prior to mixing, 2) sonication would be performed over a longer period of time to facilitate the elimination of any aggregates in solution, and 3) the diameter of the cannula used to gavage the subjects would be slightly increased. The test was continued in spite of the difficulties, as the purpose of the initial trials was to test the delivery methods and materials not to generate dose specific data. After the two test subjects had been treated, they were returned to their cages and regularly monitored throughout the remainder of the day.

Approximately 24 hours after having been dosed, both mice were found dead in their cages. The cause of death was not immediately apparent and it was decided that a standard necropsy would be performed on both animals. Tissue samples were collected and prepared

according to the previously defined experimental procedure. The results of the post mortem examination and pathology screening of the two mice can be found in Tables 22 and 23. The mouse designated R02-796 (Table 22) was dosed with 1,5-Diphenylpenta-1,4-dien-3-one (**66**) and mouse R02-797 (Table 23) was dosed with 2,6-Dibenzylidenecyclohexanone (**78**). Both subjects were found to have significant numbers of neutrophils in the sinusoids of their livers. Neutrophils are phagocytic in nature and are the principle white blood cells involved in the body's immune response to infection. The sinusoids are similar in structure and function to capillaries and are found in the liver, pancreas, spleen, and adrenal cortex. In rare instances, hepatocytes located in the centrilobular, midzonal, and subcapsular regions of the liver were observed to be anucleate, without a nucleus, or pyknotic, having a shrunken and/or hardened nucleus, in both subjects. Evidence of extensive autolysis was also observed in both animals. These results were interpreted as signs of early necrosis by the attending pathologist at the College of Veterinary Medicine. In addition, Mouse R02-797 showed signs of some abnormal fat accumulation, or lipidosis, in the liver. This, however, this was not observed in subject R02-796. The primary tumors of both mice were examined for microvessel denisity as well. Eight 400X fields were investigated for mouse R02-796. An average of 64 vessels per field was determined. Ten 400X fields were evaluated for mouse R02-797 and an average of 108 vessels was observed. In the case of both mice, multifocal cell death (necrosis) was observed within the primary tumor.

In spite of the disappointing results from the initial drug trial, a second group of mice was prepared for tumor injection and fresh drug solutions were formulated. It was decided that the concentration of the drugs would be halved (15 mg/kg) in an effort to alleviate some of the aforementioned dosing concerns. Researchers were not able to ascertain whether or not the

deaths of the original two subjects were directly related to the concentration of the drugs, but by halving the dose, it was hoped that any potential complications would be minimized. On the eleventh day of tumor development, each mouse was gavaged with 0.3 mL of a 50 mg/mL solution of a randomly assigned drug. The delivery of the compounds was straight forward and resulted in no complications. The mice were then placed in their cages and closely monitored throughout the remainder of the day. During the evening, technicians in the rodent isolation facility noticed that the animals were behaving strangely. They exhibited signs of pain and stress, indicated by moderate tail writhing. They were also observed to be lethargic and somewhat nonresponsive. This behavior was monitored over the next 36 hours and seemed to lessen as time progressed. The tail writhing had completely abated by the time the second round of treatments were scheduled to begin on day thirteen. It was decided that for the second treatment the drug concentrations would be halved once again. This resulted in solutions that were one quarter the strength of the original formulations. Each mouse was gavged with 0.3 mL of the appropriate 25 mg/mL drug solution and monitored carefully for the subsequent 24 hours. The same behavioral symptoms (pain and stress) were observed following the second drug treatment. The next morning, both mice were discovered dead in their cages.

As with the original mice, the latest test animals were subjected to post mortem, pathological analysis. The tissue and tumor samples were collected as before and the results are presented in Tables 24 and 25. The mouse designated R03-806 (Table 24) was treated with dibenzylideneacetone (**66**) and mouse R03-807 (Table 25) was treated with dibenzylidenecyclohexanone (**78**). While the original two mice (R02-796 and 797) only showed signs of abnormal cell activity in their liver tissue, the second group exhibited more widespread effects. Mouse R03-806 showed signs of pericapsular scar tissue formation in the spleen,

perilobular scar tissue in the pancreas and serosal scar tissue in the intestine. All three organs contained profuse necrotic neutrophils as well. The liver was found to have evidence of tissue hardening (mineralization) and the accumulation of translucent protein droplets. It also exhibited mild to moderate subcapsular fatty change. Hepatocyte necrosis was found to be rare however. Upon examination of the primary carcinoma, the average microvessel density over ten 400X fields was found to be 42. In addition, 90% of the primary tumor was observed to be necrotic. Similarly, mouse R03-807 exhibited signs of scar tissue formation in the pancreas (perilobular) and intestine (serosal). The intestine was also observed to contain a significant number of necrotic neutrophils. The spleen was clear of abnormalities however. The liver showed similar subcapsular fatty change to mouse R03-806, but there was also evidence of tissue death and regeneration coupled with neutrophil build up. The primary carcinoma had an average microvessel density of 78 per ten 400X fields examined. Multifocal cell death was also noted and roughly 50% of the neoplasm was found to necrotic.

The exact cause of death for each of the four test animals is still undetermined. Each of the four mice exhibited signs of mild to moderate hepatotoxicity (liver toxicity), but the pathologists did not believe that it appeared severe enough in any of the cases to ultimately kill the subjects. The hepatotoxicity was deemed to be the result of both portal uptake of the treatment compounds and their direct absorption through the hepatic capsule. At this stage of the project, it was determined that a pharmacologist was required to properly evaluate the exact concentrations and appropriate formulations of each curcumin derivative that could be safely administered to future test subjects. Unfortunately, time and money was working against the project. The primary grant funding the *in vivo* studies was expiring in a matter of months and the Veterinary School was unable to secure additional funding to enable work to continue past the

end of the spring semester (2003). It was deemed necessary to shut the project down while a pharmacologist was located and more water soluble curcumin derivatives could be synthesized and biologically evaluated. It was believed that proper pharmacological evaluation of the compounds coupled with the ability to administer the treatment solutions intravenously would greatly improve the project's chances of future success. While the results of the *in vivo* trials were ultimately disappointing, valuable experience was gained which can be directly applied to future *in vivo* studies involving the curcumin derivatives synthesized by the Bowen laboratory. The primary lesson learned as a result of the studies was in regards to dosage concentrations. It is standard procedure in biomedical research to begin *in vivo* testing using low drug dosages, not exceptionally high ones. It has been deemed expedient for future efforts to begin with very low concentrations that are gradually increased over time in order to test the tolerance levels of the test subjects. In the study described herein, the opposite methodology was implemented and the results were less that ideal. Plans to resume *in vivo* testing are still being considered at this time.

Table 22. Pathology Report for Preliminary Animal Tests – Mouse RR Cage1

Mouse	**Date Died**	**Histology Number**
RR Cage 1	Feb. 4, 2003	R02-796
Block	**Organ**	**Lesions**
1	Heart	No Histologic Lesions
	Kidney	No Histologic Lesions
	Renal lymph node	No Histologic Lesions
	Tongue	No Histologic Lesions
	Salivary gland	No Histologic Lesions
	Liver	Numerous Neutrophils in Sinusoids, Rare Anucleate and Pyknotic Hepatocytes in Centrilobular and Midzonal Regions and in Subcapsular Hepatocytes
2	Lung	Congested
	Spleen	No Histologic Lesions
	Stomach	No Histologic Lesions
	Intestine	No Histologic Lesions
	Pancreas	No Histologic Lesions
	Trachea	No Histologic Lesions
3	Primary Carcinoma	MI = 64 per 8 400X Fields (all available), Multifocal Necrosis
	Brain	Congested
	Seminal vesicles	No Histologic Lesions
	Coagulating Gland	No Histologic Lesions
	Prostate	No Histologic Lesions
	Skeletal Muscle	No Histologic Lesions
	Skin	No Histologic Lesions
	Comments	Significant Amounts of Autolysis

Table 23. Pathology Report for Preliminary Animal Tests – Mouse None Cage1

Mouse	**Date Died**	**Histology Number**
None Cage 1	Feb. 4, 2003	R02-797
Block	**Organ**	**Lesions**
1	Heart	No Histologic Lesions
	Kidney	No Histologic Lesions
	Renal lymph node	No Histologic Lesions
	Skeletal muscle	No Histologic Lesions
	Liver	Numerous Neutrophils in Sinusoids, Rare Anucleate and Pyknotic Hepatocytes in Centrilobular and Midzonal Regions and in Subcapsular Hepatocytes. Mild Lipidosis in some Centrilobular, Midzonal Hepatocytes
	Spleen	No Histologic Lesions
2	Stomach	No Histologic Lesions
	Intestine	No Histologic Lesions
	Pancreas	No Histologic Lesions
	Lung	Congested
3	Primary carcinoma	MI = 108 per 10 400X fields, Multifocal Necrosis
	Brain	Congested
	Seminal vesicles	No Histologic Lesions
	Coagulating gland	No Histologic Lesions
	Prostate	No Histologic Lesions
	Skeletal muscle	No Histologic Lesions
	Trachea	No Histologic Lesions
	Esopahgus	No Histologic Lesions
	Thyroid gland	No Histologic Lesions
	Comments	Significant Amounts of Autolysis

Table 24. Pathology Report for Preliminary Animal Tests – Mouse RR Cage2

Mouse	Date Died	Histology Number
RR cage 2	Feb 17 2003	R03-806
Block	**Organ**	**Lesions**
1	Liver	Mild to moderate subcapsular fatty change with rare necrosis, mineralization, hyaline protein droplets
	Kidney	No histologic lesions
	Spleen	Pericapsular fibrosis with frequent necrotic neutrophils
	Pancreas	Perilobular fibrosis with frequent necrotic neutrophils
	Intestine	Serosal fibrosis with frequent necrotic neutrophils
	Skeletal muscle	No histologic lesions
2	Seminal vesicles	No histologic lesions
	Coagulating gland	No histologic lesions
	Testes	No histologic lesions
	Salivary gland	No histologic lesions
	Adrenal gland	No histologic lesions
	Intestine	No histologic lesions
	Pancreas	Perilobular fibrosis with few necrotic neutrophils
	Lung	No histologic lesions
3	Brain	No histologic lesions
	Heart	No histologic lesions
	Intestine	No histologic lesions
	Pancreas	Perilobular fibrosis with few necrotic neutrophils
	Primary carcinoma	MI= 42 per 10 400X fields, over 90% of neoplasm is necrotic
	Stomach	No histologic lesions

Table 25. Pathology Report for Preliminary Animal Tests – None RR Cage2

Mouse	**Date Died**	**Histology Number**
None cage 2	Feb 17 2003	R03-807
Block	**Organ**	**Lesions**
1	Primary carcinoma	MI = 78 per 10 400X fields, multifocal necrosis (50%)
	Liver	Mild to moderate subcapsular fatty change with neutrophils, rare necrosis and regeneration
	Kidney	No histologic lesions
	Haired skin	No histologic lesions
	Pancreas	Minimal perilobular fibroplasia
2	Spleen	No histologic lesions
	Intestine	Serosal fibrosis with frequent necrotic neutrophils
	Stomach	No histologic lesions
	Lung	No histologic lesions
	Esophagus	No histologic lesions
	Trachea	No histologic lesions
3	Brain	No histologic lesions
	Heart	No histologic lesions
	Tongue	No histologic lesions
	Seminal vesicles	No histologic lesions
	Coagulating gland	No histologic lesions
	Testes	No histologic lesions

CHAPTER 4

EXPERIMENTAL DATA

Experimental Procedures

2,6-Di(pyridin-4-ylmethylene)cyclohexanone: A mixture of 4-pyridinecarboxaldehyde (1.0711 g, 0.946 mL, 10 mmol) and cyclohexanone (0.4907 g, 0.518 mL, 5 mmol) was added to approximately 20 mL of ethanol in a 50 mL round bottom flask. The resulting solution was cooled in an ice bath for several minutes until the temperature reached roughly 5°C. A 20% sodium hydroxide solution (2 mL) was then added to the solution in a dropwise fashion over the course of several minutes using an equalized addition funnel. During the base addition, the solution temperature was maintained at 5°C. After the sodium hydroxide solution was added, the resulting dark orange/yellow solution was allowed to warm to room temperature (25°C) and stirred for an additional 16 hours. At this time, the solution was neutralized with a dilute (pH = 4.0) solution of hydrochloric acid. A solid precipitate formed upon neutralization. The solid was collected and subsequently recrystallized using a minimal volume of ethanol to yield 0.213 g (15%) of the desired product as yellow crystals: mp 147-148°C (lit.[36] mp 150°C). ^{1}H NMR (400 MHz) δ 8.57-8.51 (d, 4H), 7.18-7.13 (d, 4H), 7.04 (s, 2H), 3.38-3.35 (m, 4H), 1.95-1.88 (m, 2H).

2,6-Di(pyridin-2-ylmethylene)cyclohexanone: A mixture of 2-pyridinecarboxaldehyde (10.7 g, 9.5 mL, 0.10 mol) and cyclohexanone (4.9 g, 5.2 mL, 0.05 mol) was added to 200 mL of water in a 500 mL round bottom flask. The aqueous solution was placed in an ice bath and stirred for several minutes as it cooled to roughly 5°C. A 20% sodium hydroxide solution (10 mL) was

then added dropwise to the cooled solution. The dropwise addition was made using an equalized addition funnel. A snowy white precipitate formed after the addition of the sodium hydroxide solution (thought to be the alcohol intermediate). The resulting solution was then allowed to stir for several minutes in the ice bath before being gradually warmed to room temperature and allowed to stir for approximately 24 hours. At this time 100 mL of ethanol was added to the reaction flask in an effort to dissolve the white precipitate that was formed upon the addition of the aqueous base. The precipitate remained however and stirring was continued for an additional 48 hours to ensure a complete reaction. At this point, the mixture was neutralized with approximately 100 mL of a dilute hydrochloric acid solution. A solid precipitated upon neutralization and was collected via vacuum filtration. Subsequent recrystallization with a minimal amount of ethanol afforded 8.98 g (53%) of the pure product as bright yellow needles: mp 125-126.5°C (lit.[37] mp 127°C). ^{1}HNMR (400 MHz) δ 8.70-8.69 (d, 2H), 7.74-7.68 (m, 4 H), 7.45-7.42 (d, 2 H), 7.22-7.17 (m, 2 H), 3.32-3.27 (t, 4 H), 1.86-1.78 (m, 2 H).

2-Benzylidene-6-pyridin-2-ylmethylenecyclohexanone: To a 3 mL conical vial (microscale) containing 1 mL of a stirring 5.5% sodium hydroxide /ethanol/water solution (10 g NaOH, 100mL water, 75 mL ethanol) was added one equivalent of 2-pyridinecarboxaldehyde (0.044 g, 46.7 μL, 0.5 mmol), one equivalent of benzaldehyde (0.0521 mL, 49.89 μL, 0.5 mmol) and one equilavent of acetone (0.028 g, 36 μL, 0.5 mmol). The resulting solution was allowed to stand at room temperature, with occasional stirring, for 30 minutes. A yellow solid precipitated and was collected via vacuum filtration and washed with several aliquots of ice cold water. TLC analysis indicated three different product spots. These spots corresponded to the dibenzyl, dipyridyl and the desired, mixed benzyl/pyridyl product. Column chromatography with silica gel using 1:1

hexanes:ethyl acetate was used to isolate the desired product as light yellow crystals. The reaction afforded 53 mg (44.9%) of the pure product: mp 120-121°C. ^{1}HNMR (400 MHz) δ 8.62-8.63 (d, 1H), 7.55-7.61 (m, 2H), 7.49-7.50 (d, 1H), 7.21-7.38 (m, 6H), 1.93-1.96 (t, 4H), 1.35-1.37 (m, 2H).

1,5-Bis(2,6-dimethoxyphenyl)penta-1,4-dien-3-one: 2,6-dimethoxycarboxaldehyde (500 mg, 3.0 mmol) and acetone (87 mg, 0.110 mL, 1.5 mmol) were added to a small volume of methanol (3.5 mL). The solution was stirred for several minutes to ensure the complete dissolution of the starting materials. When the round bottom flask containing the reaction mixture was added to an ice bath in order to lower its temperature to 5°C, the dicarboxaldehyde precipitated. For this reason, the reaction flask was removed from the bath and allowed to react at room temperature. 1 mL of a 40% sodium hydroxide solution was then added to the flask in a dropwise fashion over several minutes. The resulting solution became cloudy and light yellow after the base addition and was allowed to stir for approximately 16 hours. A light yellow precipitate formed and was subsequently collected via vacuum filtration. The crude product was then recrystallized using a minimal amount of methanol to afford 194 mg (36.5%) of the pure product as light yellow crystals: mp 143-145 °C. ^{1}HNMR (400 MHz) δ 8.10-8.15 (d, 2H), 7.45-7.56 (d, 2H), 7.15-7.19 (d, 2H), 6.25-6.29 (d, 4H), 3.72-3.76 (s, 12H).

1,5-Di(naphthalen-2-yl)penta-1,4-dien-3-one: To a flask containing a stirred aliquot of ethanol (7.5 mL) was added 2-napthylaldehyde (1.56 g, 10.0 mmol) and acetone (290 mg, 0.367 mL, 5.0 mmol). The resulting solution was added to an ice bath and 5 mL of a 40% sodium hydroxide solution was added dropwise over several minutes. After two drops of the basic solution was

added to the reaction flask, the solution became viscous and congealed. 10 mL of ethanol was added in order to dilute the thick mass. The yellow/white slurry was allowed to stir for approximately 16 hours at room temperature. TLC of the reaction pot using an 8:2 hexanes:ethyl acetate solution indicated a complete reaction. The precipitate was filtered via vacuum filtration and the impure product was collected as a light yellow powder. Subsequent recrystallization with ethyl acetate resulted in 1.464 g (43.8%) of the pure product as light yellow crystals: mp 242-245°C (lit.[38] mp 243-244°C). ^{1}HNMR (400 MHz) δ 7.31 (d, 2 H), 7.55-7.65 (m, 5 H), 7.80-8.01 (m, 9 H), 7.99 (d, 2 H).

1,5-Di(naphthalen-1-yl)penta-1,4-dien-3-one: 1-Napthylaldehyde (1.56 g, 1.356 mL, 10.0 mmol) and acetone (290 mg, 0.367 mL, 5.0 mmol) were each added to a 50 mL round bottom flask containing approximately 10 mL of ethanol. The resulting light yellow solution was stirred and added to an ice bath and subsequently cooled to approximately 5°C prior to further reaction. At this point, 1.5 mL of a 10% sodium hydroxide solution was added dropwise to the stirring solution over the course of several minutes. Solid began to form after approximately 3 minutes. The deep yellow solution was removed from the ice bath and allowed to stir at room temperature for approximately 24 hours. The precipitate was isolated via vacuum filtration and subsequently recrystallized from ethyl acetate to afford 329 mg (19.7%) of the pure product as a canary yellow powder: mp 130-132°C (lit.[38] mp 128°C). ^{1}HNMR (400 MHz) δ 7.30 (d, 2 H), 7.51-7.65 (m, 6 H), 7.89-7.95 (m, 6 H), 8.29-8.31 (m, 2 H), 8.67 (d, 2 H).

2,6-Di(2-chloro-6-fluorobenzylidene)cyclohexanone: Cyclohexanone (491 mg, 0.518 mL, 5.0 mmol) and ethanol (15 mL) were added to a 50 mL round bottom flask and allowed to stir as 2-

chloro-6-fluoro-benzaldehyde (1.58 g, 10.0 mmol) was slowly added. The resulting solution was cooled in an ice bath (5°C) and allowed to stir for several minutes. A 5 mL aliquot of a 40% sodium hydroxide solution was then added dropwise to the flask via an equalized addition funnel over several minutes. The solution began to show signs of precipitate formation almost immediately. The flask was then allowed to warm to room temperature and stir for approximately 4 hours. The solid was collected at this time via vacuum filtration. Subsequent recrystallization of the crude product from ethanol afforded 1.44 g (76.2%) of the pure product as bright yellow crystals: mp 118-119 °C. ^{1}HNMR (400 MHz) δ 7.65-7.66 (s, 2H), 7.26-7.34 (m, 4H), 7.01-7.11 (d, 2H), 2.51-2.60 (t, 4H), 1.49-1.52 (m, 2H).

1,5-Di(anthracen-9-yl)penta-1,4-dien-3-one: To a small volume of ethanol (40 mL) in a 100 mL round bottom flask was added 9-anthraldehyde (1.03 g, 5.0 mmol). The resulting mixture was heated gently to facilitate complete dissolution of the 9-anthryl starting material. The solution was cooled to room temperature and acetone (145.2 mg, 0.184 mL, 2.5 mmol) was added and the solution was allowed to stir for several minutes. A small portion of a 40% potassium hydroxide solution (2.3 mL) was then added to the reaction flask in a dropwise fashion over several minutes using a self equalizing addition funnel. The solution became dark orange upon the initial addition of the potassium hydroxide solution. After several minutes, it began to thicken and solid was visible in the solution. The reaction mixture was allowed to stir at room temperature for an additional 6 hours. At this time, TLC analysis of the mixture using 8:2 hexanes:ethyl acetate indicated that there was no starting material remaining in the reaction solution. The crude solid product was collected via vacuum filtration. Subsequent recrystallization utilizing ethyl acetate afforded 1.04 g (47.9%) of the pure product as light

yellow crystals: mp 275-277 °C. ^{1}HNMR (400 MHz) δ 7.91-8.19 (m, 10H), 7.66-7.75 (d, 2H), 7.39-7.45 (d, 8H), 7.03-7.10 (d, 2H).

2,6-Di(anthracen-9-ylmethylene)cyclohexanone: A small amount of 9-Anthraldehyde (0.412 g, 2.0 mmol) was dissolved in approximately 20 mL of gently heated ethanol in a 50 mL round bottom flask. Heat was necessary to affect the complete dissolution of the 9-napthyl starting material. Next, cyclohexanone (0.98 g, 0.103 mL, 1 mmol) was added to the stirring solution. The reaction mixture was allowed to cool to room temperature before 5 mL of 40% potassium hydroxide was added dropwise over several minutes via a self equalizing addition funnel. The solution turned a dark yellow/brown upon addition of the basic solution. Solid became evident in the solution within a matter of minutes. The solution was allowed to stir at room temperature for approximately 24 hours after a TLC assessment after 2 hours showed signs of starting material in the reaction flask. At this point a yellow precipitate was evident in the flask and the solution was filtered to obtain the crude product. Subsequent recrystallization from ethyl acetate afforded 287 mg (60.4%) of the pure product as a canary yellow powder: mp 290-292 °C. ^{1}HNMR (400 MHz) δ 7.89-8.10 (m, 10H), 7.69-7.74 (d, 2H), 7.30-7.39 (d, 8H), 6.98-7.05 (d, 2H), 2.15-2.18 (t, 2H), 1.30-1.33 (m, 2H).

1,5-Diphenylpenta-1,4-dien-3-one: Benzaldehyde (0.104 g, 100 μL, 1.0 mmol) was combined with acetone (0.028 g, 36 μL, 0.5 mmol) in a 3 mL conical vial (microscale). A 1 mL aliquot of a 5.5% NaOH ethanolic solution prepared from 1.0 g sodium hydroxide, 10 mL water and 7.5 mL ethanol was added to the vial in a dropwise fashion. The solution was allowed to stand at room temperature for approximately one hour with occasional agitation. A light yellow

precipitate was observed and was isolated via vacuum filtration. The crystals were washed with three 1 mL portions of ice cold water in order to remove impurities and neutralize any residual sodium hydroxide. The crude product was subsequently recrystallized from ethanol to afford 93 mg (80%) of light yellow needles: mp 110-111°C (lit.[39] mp 110-111°C). ^{1}HNMR (400 MHz) δ 7.78-7.74 (d, 2 H), 7.65-7.62 (m, 4H), 7.44-7.42 (m, 6 H), 7.12-7.08 (d, 2 H).

2,6-Dibenzylidenecyclohexanone: Benzaldehyde (0.104 g, 100 μL, 1.0 mmol) was combined with cyclohexanone (0.048 g, 51 μL, 0.5 mmol) in a 3 mL conical vial (microscale). A 1 mL aliquot of a 5.5% sodium hydroxide ethanolic solution prepared from 1.0 g sodium hydroxide, 10 mL water and 7.5 mL ethanol was added to the vial in a dropwise fashion. The solution was allowed to stand at room temperature for approximately 45 minutes with recurrent agitation. No precipitate was evident after 45 minutes so 2 mL of water was added to the vial. A light white/yellow precipitate was forced out of solution upon that addition of water and was isolated via vacuum filtration. The crystals were washed with three 1 mL portions of ice cold water in order to remove impurities and neutralize any residual sodium hydroxide. The crude product was then recrystallized from ethanol to afford 85 mg (62%) of light yellow needles: mp 115-116°C (lit.[39] mp 116-117°C). ^{1}HNMR (400 MHz) δ 7.82 (s, 2 H), 7.49-7.47 (d, 4H), 7.44-7.40 (t, 4 H), 7.37-7.34 (t, 2 H), 2.97-2.93 (t, 4 H), 1.84-1.77 (m, 2 H).

1-Anthracen-9-yl-3-naphthalen-2-ylpropenone: Individual portions of 2-napthaldehyde (355 mg, 2.27 mmol) and 9-acetylanthracene (500 mg, 2.27 mmol) were combined in a 50 mL round bottom flask containing approximately 10 mL of ethanol. The flask was placed in an ice bath and allowed to stir as the solution cooled to 10°C over several minutes. A 1 mL portion of a

40% potassium hydroxide solution was slowly added to the reaction flask in a dropwise fashion using a self equalizing addition funnel. After the basic solution was added, the flask was allowed to warm to room temperature and stir for approximately 45 minutes. At this time, a thick, yellow gum had formed within the flask. The viscous product was collected via vacuum filtration and subsequently recrystallized from a minimal amount of ethanol to afford 530 mg (65%) of a bright yellow powder: mp 157-158°C. ^{1}HNMR (400 MHz) δ 8.58 (s, 1 H), 8.12-8.07 (m, 2 H), 8.01-7.97 (m, 2 H), 7.83-7.66 (m, 5 H), 7.55-7.42 (m, 8 H).

1,3-Diphenylpropynone: To a stirring solution[40] of phenylacetylene (0.306 g, 0.329 mL, 3.0 mmol) and 9 mL of triethylamine under an inert nitrogen atmosphere was added 0.0286 g of copper (I) iodide (0.15 mmol). Benzoyl chloride (0.527 g, 0.435 mL, 3.75 mmol) was then carefully added to the reaction flask in a dropwise fashion using a self equalizing addition funnel which had been fitted with a rubber septum and a direct connection to the nitrogen source in order to ensure that the inert atmosphere was undisturbed. The system was then allowed to stir at room temperature for approximately 30 hours. The triethylamine was then removed from the flask using a water aspirator and gentle heating (heat gun). The reaction residue was then diluted with approximately 3 mL of methanol and allowed to stir for an additional 5-10 minutes. The methanol was subsequently removed using a rotoevaporator. The resulting light yellow viscous oil was then dissolved in 50 mL of chloroform and washed three times with 15 mL aliquots of deionized water to remove any salt by-products formed during the course of the reaction. The chloroform layer was then isolated, dried with sodium sulfate and concentrated under reduced pressure. The crude product was a dark orange oil. Column chromatography with silica gel using a 9:1 methylene chloride:ethanol solvent system was used to obtain 142 mg (23%) of the

pure product as a dark yellow oil. ^{1}HNMR (400 MHz) δ 8.18-8.16 (d, 2 H), 7.70-7.66 (t, 1 H), 7.62-7.60 (d, 2 H), 7.55-7.52 (t, 2 H), 7.50-7.45 (m, 3 H).

(4-Allyloxyphenyl)-(2-allyloxyphenyl)methanone: To a stirred solution[41] of (2-hydroxyphenyl)-(4-hydroxyphenyl)methanone (0.214 g, 1.0 mmol) and acetone (10 mL) was added potassium carbonate (0.552 g, 4.0 mmol) and allyl bromide (0.242 g, 190.3 μL, 2.0 mmol). The reaction mixture was heated to reflux for approximately 6 hours. At this point, the flask was slowly cooled to room temperature and gravity filtered in order to remove the potassium carbonate and potassium bromide present in the mixture. The filtrate was then concentrated under reduced pressure to obtain the crude product as a thin yellow oil. The oil was purified via column chromatography with silica gel using a 9:1 hexanes:ethyl acetate solvent system. The pure product (191 mg, 65%) was obtained as a clear, viscous oil. ^{1}HNMR (400 MHz) δ 7.3-7.6 (m, 4 H), 6.45-6.6 (d, 4 H), 6.0-6.17 (q, 1 H), 5.6-5.75 (q, 1 H), 5.3-5.55 (dd, 2 H), 4.9-5.1 (dd, 2 H), 4.5-4.65 (d, 2 H), 4.3-4.4 (d, 2 H).

REFERENCES

1. MedlinePlus: Medical Dictionary. http://www.nlm.nih.gov/medlineplus/mplusdictionary.html (accessed April 2005).
2. Szekanecz, Z.; Joon, A. E.; *Recent Research Developments in Immunology* **2002,** 4(pt.2), 523.
3. Takagi, H. *Saishin Igaku* **2001,** 56(8), 1792.
4. Folkman, J. *Ann. Surg.* **1972,** 175, 409-416.
5. Folkman, J.; Bach, M.; Rowe, J. W.; Davidoff, F.; Lambert, P.; Hirsch, C.; Goldberg, A.; Hiatt, H. H.; Glass, J.; Henshaw, E. *N. Engl. J. Med.* **1971**, 285, 1182-1186.
6. Ammon, H. P.; Wahl, M. *Planta Med*. **1991**, 57, 1.
7. Stoner, G. D.; Mukhtar, H. *J. Cell. Biochem. Suppl.* **1995**, 22, 169.
8. Sharma, O. P. *Biochem. Pharmacol.* **1976**, 25, 1811.
9. Toda, S.; Miyase, T,; Arichi, H.; Tanizawa, H.; Takiyano, Y. *Chem. Pharm.* **1985**, 33, 1725.
10. Srimal, R. C.; Dhawan, B. N. *J. Pharm. Pharmacol.* **1973**, 25, 447.
11. Satoskar, R. R.; Shah, S. J.; Shenoy, S. G. *Int. J. Clin. Pharmacol. Ther. Toxicol.* **1986**, 24, 651.
12. Mazumder, A.; Raghavan, K.; Weinstein, J.; Kohn, K. W.; Pommer, Y. *Biochem. Pharmacol.* **1995**, 49, 1165.
13. Eigner, D.; Scholz, D. *J. Ethnopharmacol.* **1999**, 67, 1.

14. Huang, M. T.; Lou, Y. R.; Ma, W.; Newmark, H. L.; Reuhl, K. R.; Conney, A. R. *Cancer Res.* **1994**. 54, 5841.

15. Rao, C. V.; Rivenson, A.; Simi, B.; Reddy, B. S. *Cancer Res.* **1995**, 55(2), 259.

16. Conney, A. H.; Lysz, T.; Ferraro, T.; Abidi, T. F.; Manchand, P. S.; Laskin, J. D.; Huang, M. T. *Adv. Enzyme Regul.* **1991**, 31, 385.

17. Huang, M. T.; Ma, W.; Lu, Y. P.; Chang, R. L.; Fisher, C.; Manchand, P. S.; Newmark, H. L.; Conney, A. H. *Carcinogenesis* **1995**, 16, 2493.

18. Huang, M. T.; Deschner, E. E.; Newmark, H. L.; Wang, Z. Y.; Ferraro, T. A.; Conney, A. H. *Cancer Lett.* **1992**, 64, 117.

19. Arbiser, J. L.; Klauber, N.; Rohan, R.; van Leeuwen, R.; Huang, M. T.; Fisher, C.; Flynn, E.; Byers, H. R. *Molecular Medicine* **1998**, 4, 376.

20. Robinson, T. P.; Ehlers, T.; Hubbard, R. B.; Bai, X. H.; Arbiser, J. L.; Goldsmith, D. J.; Bowen, J. P. *Bioorg. Med. Chem. Lett.* **2003**, 13(1): 115.

21. Furness, M. S.; Robinson, T. P.; Ehlers, T.; Hubbard, R. B., IV; Arbiser, J. L.; Goldsmith, D. J.; Bowen, J. P. *Current Pharmaceutical Design* **2005**, 11(3), 357.

22. Bowen, J. P.; Robinson, T. P.; Ehlers, T.; Goldsmith, D.; Arbiser, J. Chalcone and its analogs as agents for the inhibition of angiogenesis and related disease states. PCT Int. Appl. WO0146110, **June 28, 2001**.

23. Nielson, A. T.; Houlihan, W. J. Org. React. **1968**, 16,1.

24. Arbiser, J. L.; Moses, M. A.; Fernandez, C. A.; Ghiso, N.; Cao, Y.; Klauber, N.; Frank, D.; Brownlee, M.; Flynn, E.; Parangi, S.; Byers, H. R.; Folkman, J. *Proc. Natl. Acad. Sci. U.S.A.* **1997**, 94(3), 861.

25. Jat, P. S.; Sharp, P. A. *Moll. Cell. Biol.* **1989**, 9, 1672.

26. Voyta, J. C.; Via, D. P.; Butterfield, C. E.; Zetter, B. R. *J. Cell Biol.* **1984,** 99, 2034.

27. Dotto, G. P.; Parada, L. F.; Weinberg, R. A. *Nature (London)*. **1985**, 318, 472.

28. Dhar, R.; Ellis, R. W.; Shih, T. Y.; Oroszlan, S.; Shapiro, B.; Maizel, J.; Lowy, D.; Scolnick, E. *Science*. **1982**, 217, 934.

29. Cornell, K. K.; Bostwick, D. G.; Cooley, D. M.; et al. *The Prostate* **2000**, 45, 173.

30. Vail, D. M.; MacEwen, E. G. *Cancer Investigation* **2000**, 18, 781.

31. Straw, R. C. Tumors of the skeletal system. In: Withrow, S. J. and MacEwan, E. G. eds. Small Animal Clinical Oncology. 2nd Ed. Philadelphia, **1996**: 287.

32. Chun, R.; Kurzman, I. D.; Couto, C. G.; et al. *J. Vet. Intern Med.* **2000**, 14, 495.

33. Shoieb, A. M.; Hahn, K. A.;Barnhill, M. A. *In Vivo* **1998**, 12, 463.

34. Cattoretti, G.; Suurmeijer, A. J. H. *Adv. Anatomic Pathol.* **1994**, 2, 2.

35. Shi, S-R.; et al. *J. Histotech. Cytochem.* **1991**, 39, 741.

36. Buh-Hoi, N. P.; Xuong, N. D. *Compt. Rend.* **1960**, 251, 2725.

37. Harries, C.; Lenhart, H. *Justus Liebigs Ann. Chem.* **1915**, 410, 113.

38. Seifert, M.; Kuck, D. *Tetrahedron* **1996**, 52(41), 13167.

39. Hill, R. K.; Barbaro, J. Experiments in Organic Chemistry Contemporary Publishing Co. of Raleigh, Inc.: Raleigh, **1996**, E12-1.

40. Chowdhury, C.; Kundu, N. G. *Tetrahedron* **1999**, 55, 7011.

41. Mereyala, H. B.; Gurrala, S. R.; Mohan, S. K. *Tetrahedron* **1999**, 55, 11331.

Appendix A – Total Cell Count Data for DMSO Controls

Appendix A: Total Cell Count Data for DMSO Controls

Compound	DMSO Control Cell Count Data			
	1 µg/ml	3 µg/ml	6 µg/ml	9 µg/ml
1,3-Diphenylpropenone (1)	171880	141380	128640	----
1-(4-Chlorophenyl)-3-p-tolylpropenone (2)	171880	141380	128640	----
3-(2,6-Dichlorophenyl)-1-p-tolylpropenone (3)	171880	141380	128640	----
3-(2,4-Dichlorophenyl)-1-p-tolylpropenone (4)	171880	141380	128640	----
3-(4-Isopropylphenyl)-1-p-tolylpropenone (5)	171880	141380	128640	----
3-(2,6-Dimethylphenyl)-1-phenylpropenone (6)	171880	141380	128640	----
1,3-Di-p-tolylpropenone (7)	171880	141380	128640	----
1-(2,4-Dimethylphenyl)-3-phenylpropenone (8)	171880	141380	128640	----
3-(2-Chlorophenyl)-1-(2,4-dimethylphenyl)propenone (9)	171880	141380	128640	----
1,3-Di(4-chlorophenyl)propenone (10)	171880	141380	128640	----
3-Phenyl-1-(3-trifluoromethylphenyl)propenone (11)	171880	141380	128640	----
3-(4-Chlorophenyl)-1-p-tolylpropenone (12)	171880	141380	128640	----
1,3-Bis(2,6-dichloro-phenyl)propenone (13)	186140	340720	221080	374340
1-(4-Aminophenyl)-3-(3-aminophenyl)propenone (14)	1573200	1573200	1573200	1573200
1,3-Di(4-methoxyphenyl)propenone (15)	1711880	141380	128640	----
3-(2,6-Dichlorophenyl)-1-phenylpropenone (16)	171880	141380	128640	----
1-(2,6-Dichlorophenyl)-3-phenylpropenone (17)	102040	102040	102040	----
3-(2,6-Dichlorophenyl)-1-(2,6-dimethoxyphenyl)propenone (18)	178800	154880	142200	----
3-(2,6-Dimethoxyphenyl)-1-phenylpropenone (19)	178800	154880	142200	----
1-(2,6-Dimethoxyphenyl)-3-phenylpropenone (20)	178800	154880	142200	----
1,3-Bis(2,6-dimethoxyphenyl)propenone (21)	178800	154880	142200	----
1-Phenyl-3-pyridin-2-ylpropenone (22)	102040	102040	102040	----
1-Phenyl-3-pyridin-3-ylpropenone (23)	102040	102040	102040	----
1,3-Dipyridin-2-ylpropenone (24)	102040	102040	102040	----
1-Pentamethylphenyl-3-phenylpropenone (25)	178800	154880	142200	----
1-(4-carboxymethylphenyl)-3-phenylpropenone (26)	171880	141380	128640	----
1,3-Bispentafluorophenylpropenone (27)	----	----	----	----
3-(4-Nitro-phenyl)-1-phenylpropenone (28)	1573200	1573200	1573200	1573200
3-Pentafluorophenyl-1-phenylpropenone (29)	----	----	----	----
1-Pentafluorophenyl-3-phenylpropenone (30)	----	----	----	----
1,3-Diphenylpropan-1-one (31)	60880	60650	66900	57020
1,3-Diphenylpropynone (32)	333400	261360	269480	269920
1-Naphthalen-2-yl-3-phenylpropenone (33)	60880	60650	66900	57020
3-Naphthalen-2-yl-1-phenylpropenone (34)	186140	340720	221080	374340

Appendix A: Total Cell Count Data for DMSO Controls (continued)

Compound	DMSO Control Cell Count Data			
	1 µg/ml	3 µg/ml	6 µg/ml	9 µg/ml
1-Biphenyl-4-yl-3-phenylpropenone (35)	178800	154880	142200	----
1,3-Bis-biphenyl-4-ylpropenone (36)	178800	154880	142200	----
3-Biphenyl-4-yl-1-phenylpropenone (37)	178800	154880	142200	----
3-(2,6-Dichlorophenyl)-1-naphthalen-2-ylpropenone (38)	186140	340720	221080	374340
3-(4-Benzyloxyphenyl)-1-(4-chlorophenyl)propenone (39)	171880	141380	128640	----
3-(4-Benzyloxyphenyl)-1-p-tolylpropenone (40)	171880	141380	128640	----
1-Anthracen-9-yl-3-phenylpropenone (41)	178800	154880	142200	----
3-Anthracen-9-yl-1-phenylpropenone (42)	178800	154880	142200	----
1-Anthracen-9-yl-3-naphthalen-2-ylpropenone (43)	178800	154880	142200	----
1-Naphthalen-1-yl-3-phenylpropenone (44)	178800	154880	142200	----
1,3-Dianthracen-9-ylpropenone (45)	102040	102040	102040	----
3-Naphthalen-1-yl-1-naphthalen-2-ylpropenone (46)	102040	102040	102040	----
3-Naphthalen-2-yl-1-naphthalen-1-ylpropenone (47)	102040	102040	102040	----
1,3-Dinaphthalen-1-ylpropenone (48)	102040	102040	102040	----
3-Benzo[1,3]dioxol-5-yl-1-(3,4-dimethoxyphenyl)propenone (49)	139680	144660	145560	146620
3-Benzo[1,3]dioxol-5-yl-1-naphthalen-2-ylpropenone (50)	139680	144660	145560	146620
3-Benzo[1,3]dioxol-5-yl-1-p-tolylpropenone (51)	139680	144660	145560	146620
3-Benzo[1,3]dioxol-5-yl-1-(4-methoxyphenyl)propenone (52)	139680	144660	145560	146620
3-Benzo[1,3]dioxol-5-yl-1-(2-hydroxyphenyl)propenone (53)	191360	155500	137400	165540
3-Benzo[1,3]dioxol-5-yl-1-phenylpropenone (54)	191360	155500	137400	165540
3-Benzo[1,3]dioxol-5-yl-1-pyridin-3-ylpropenone (55)	191360	155500	137400	165540
3-Benzo[1,3]dioxol-5-yl-1-pyridin-2-ylpropenone (56)	191360	155500	137400	165540
1,3-Difuran-2-ylpropenone (57)	178800	154880	142200	----
3-Furan-2-yl-1-phenylpropenone (58)	178800	154880	142200	----
1-Furan-2-yl-3-phenylpropenone (59)	102040	102040	102040	----
3-Phenyl-1-(1H-pyrrol-2-yl)propenone (60)	102040	102040	102040	----
1-Phenyl-3-(1H-pyrrol-2-yl)propenone (61)	102040	102040	102040	----
2-Benzylidene-3,4-dihydro-2H-naphthalen-1-one (62)	186140	340720	221080	374340
2-(2,6-Dichlorobenzylidene)-3,4-dihydro-2H-naphthalen-1-one (63)	102040	102040	102040	----
2-Naphthalen-2-ylmethylene-3,4-dihydro-2H-naphthalen-1-one (64)	60880	60650	66900	57020
2-Naphthalen-1-ylmethylene-3,4-dihydro-2H-naphthalen-1-one (65)	60880	60650	66900	57020
1,5-Diphenylpenta-1,4-dien-3-one (66)	333400	261360	269480	269920
1,5-Bis(2-chloro-6-fluorophenyl)penta-1,4-dien-3-one (67)	178800	154880	142200	----
1,5-Bis(2,6-dichlorophenyl)penta-1,4-dien-3-one (68)	178800	154880	142200	----

Appendix A: Total Cell Count Data for DMSO Controls (continued)

Compound	DMSO Control Cell Count Data			
	1 µg/ml	3 µg/ml	6 µg/ml	9 µg/ml
1,5-Bis(2,6-dimethoxyphenyl)penta-1,4-dien-3-one (69)	31640	29380	24760	28000
1,5-Bis(4-dimethylaminophenyl)penta-1,4-dien-3-one (70)	1617480	1617480	1617480	1617480
1,5-Difuran-2-ylpenta-1,4-dien-3-one (71)	102040	102040	102040	----
1,5-Bisbenzo[1,3]dioxol-5-ylpenta-1,4-dien-3-one (72)	139680	144660	145560	146620
1-Benzo[1,3]dioxol-5-yl-5-phenylpenta-1,4-dien-3-one (73)	191360	155500	137400	165540
1,5-Bis(naphthalen-2-yl)penta-1,4-dien-3-one (74)	31640	29380	24760	28000
1,5-Bis(naphthalen-1-yl)penta-1,4-dien-3-one (75)	31640	29380	24760	28000
1,5-Bis(anthracen-9-yl)penta-1,4-dien-3-one (76)	31640	29380	24760	28000
2,5-Dibenzylidenecyclopentanone (77)	171880	141380	128640	----
2,6-Dibenzylidenecyclohexanone (78)	333400	261360	269480	269920
2,6-Bis(2,6-dichlorobenzylidene)cyclohexanone (79)	102040	102040	102040	----
2,6-Di(2-chloro-6-fluorobenzylidene)cyclohexanone (80)	295746.7	306246.7	291186.7	298930
2,6-Di(pyridin-2-ylmethylene)cyclohexanone (81)	333400	261360	269480	269920
2-Benzylidene-6-pyridin-2-ylmethylenecyclohexanone (82)	1462920	1432680	1334680	1413680
2,6-Di(pyridin-4-ylmethylene)cyclohexanone (83)	333400	261360	269480	269920
2,6-Di(4-hydroxy-3-methoxybenzylidene)cyclohexanone (84)	1573200	1573200	1573200	1573200
2,6-Di(naphthalen-1-ylmethylene)cyclohexanone (85)	102040	102040	102040	----
2,6-Di(naphthalen-2-ylmethylene)cyclohexanone (86)	102040	102040	102040	----
2,6-Di(anthracen-9-ylmethylene)cyclohexanone (87)	31640	29380	24760	28000
3,5-Di(4-hydroxy-3-methoxybenzylidene)tetrahydropyran-4-one (88)	1617480	1617480	1617480	1617480

Appendix B – Representative ^{1}H NMR Spectra

2,6-Di(pyridine-4-ylmethylene)cyclohexanone

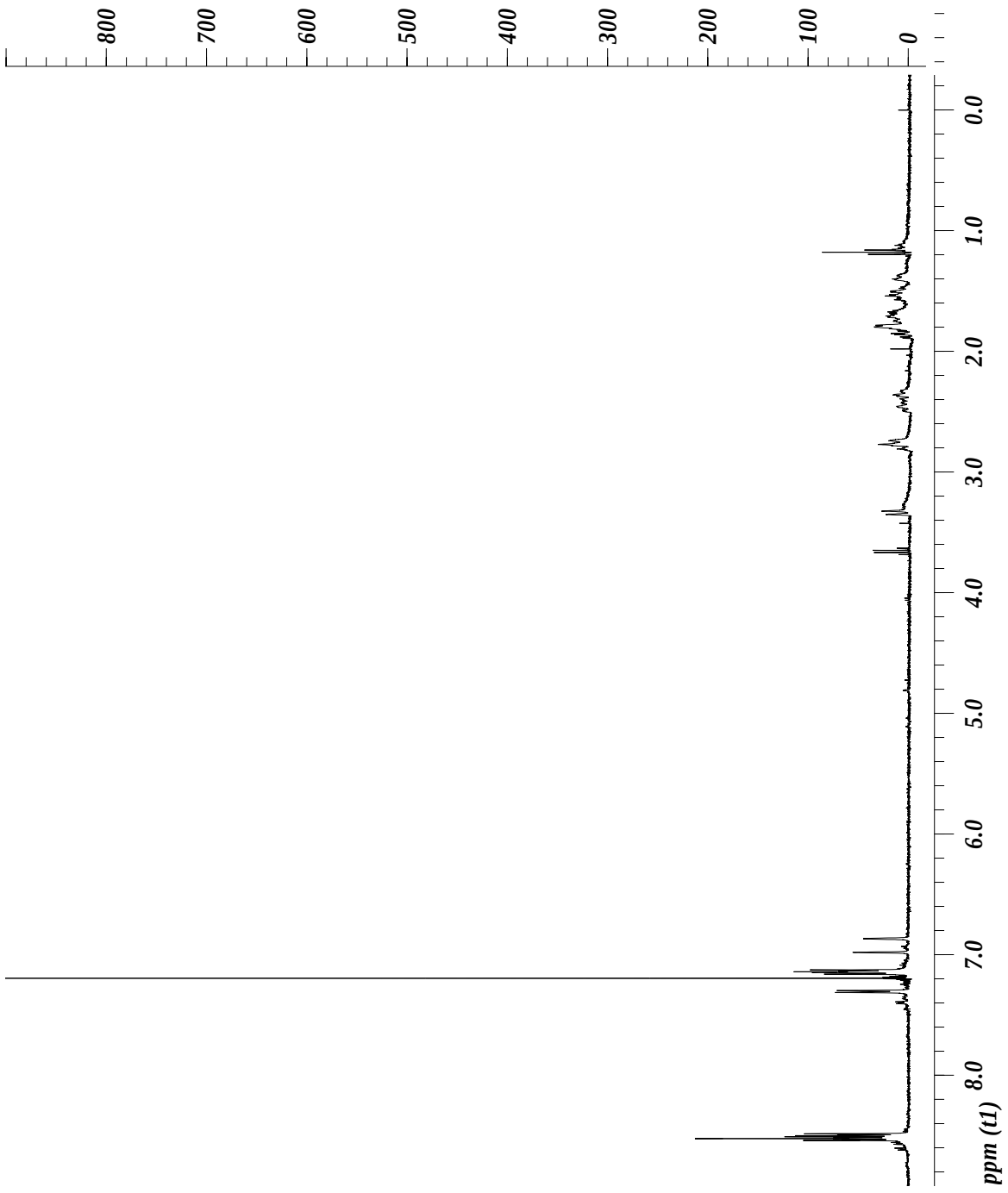

2,6-Di(pyridine-2-ylmethylene)cyclohexanone

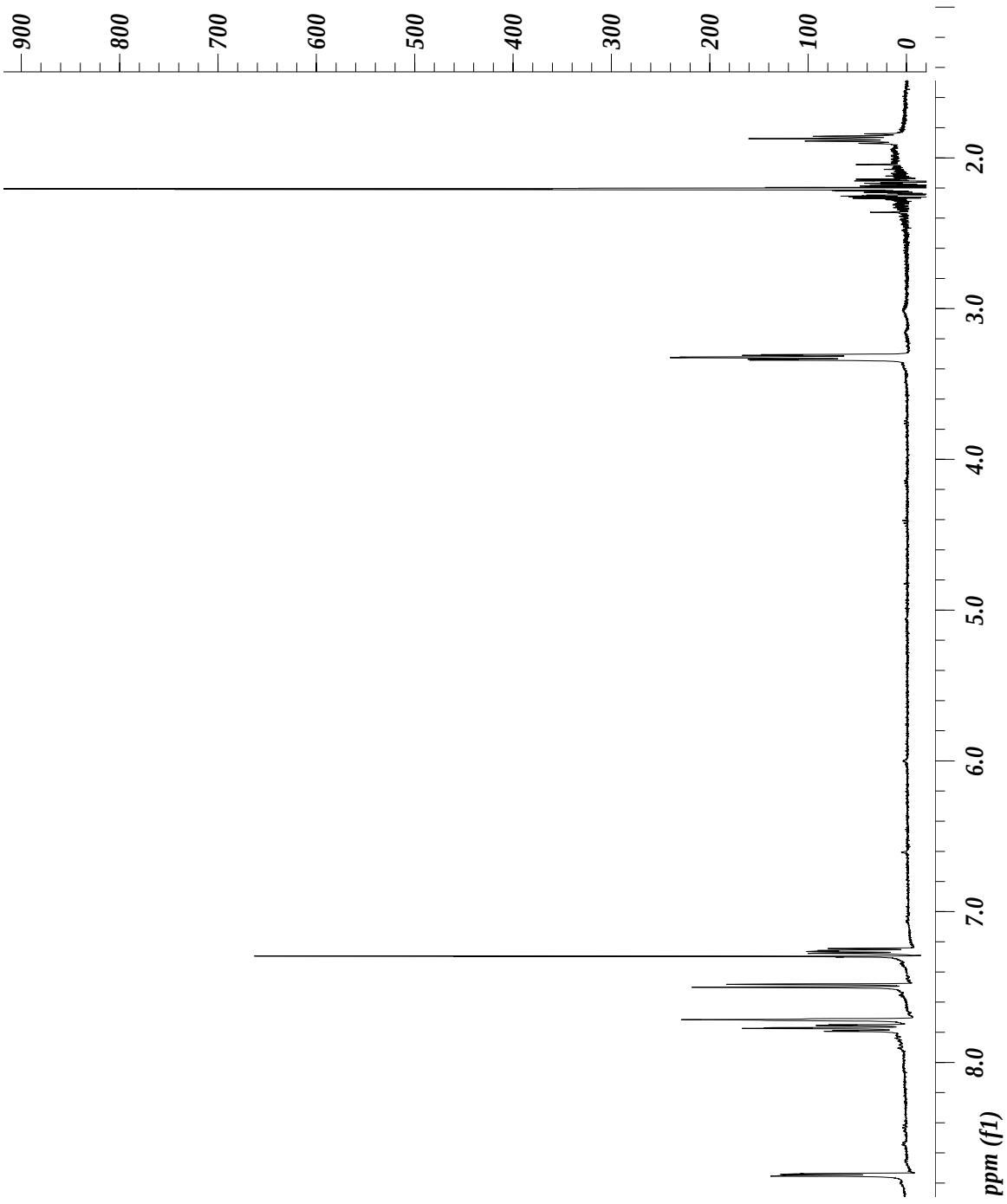

1,5-Bis(2,6-dimethoxyphenyl)penta-1,4-dien-3-one

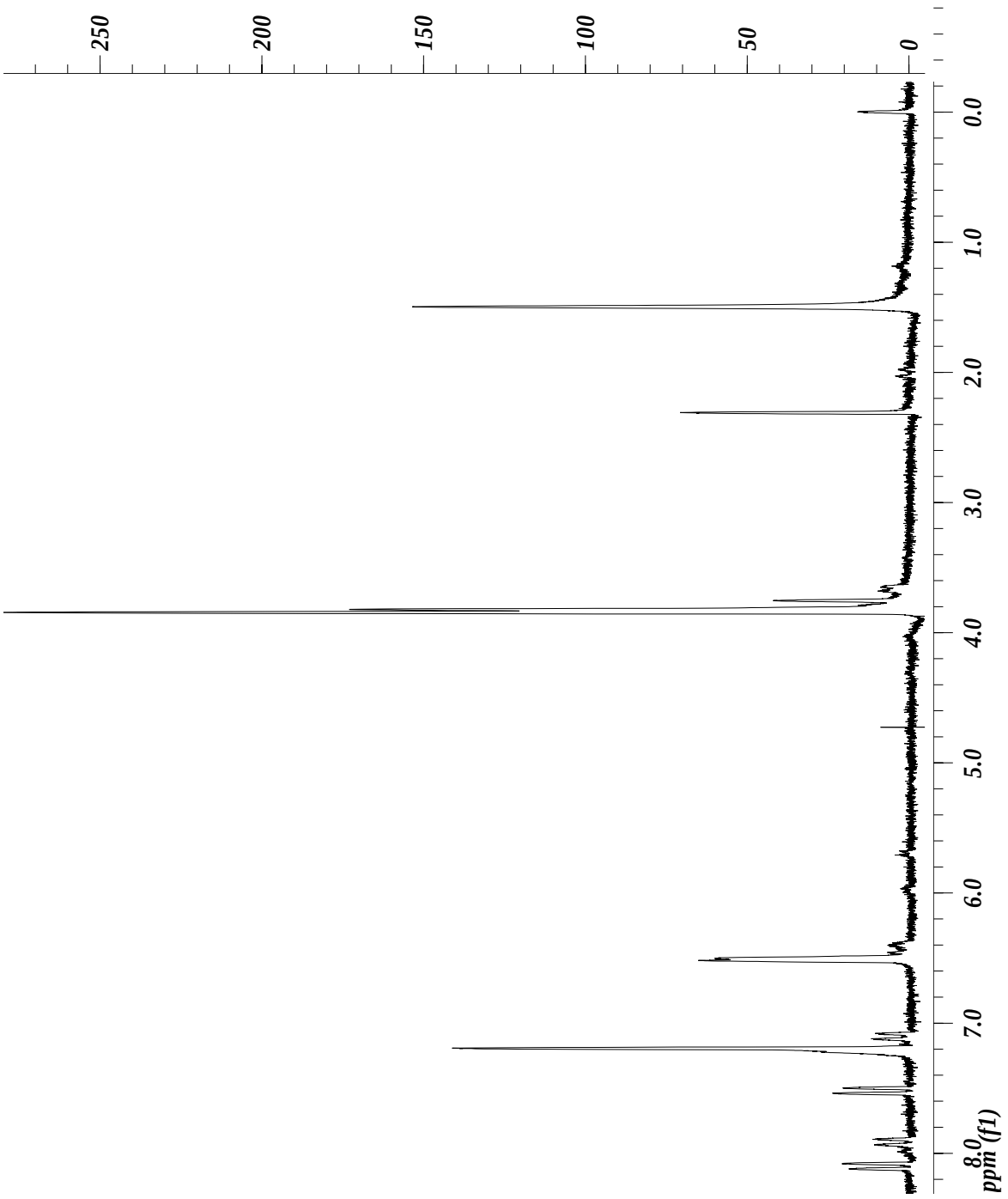

1,5-Di(napthalen-2-yl)penta-1,4-dien-3-one

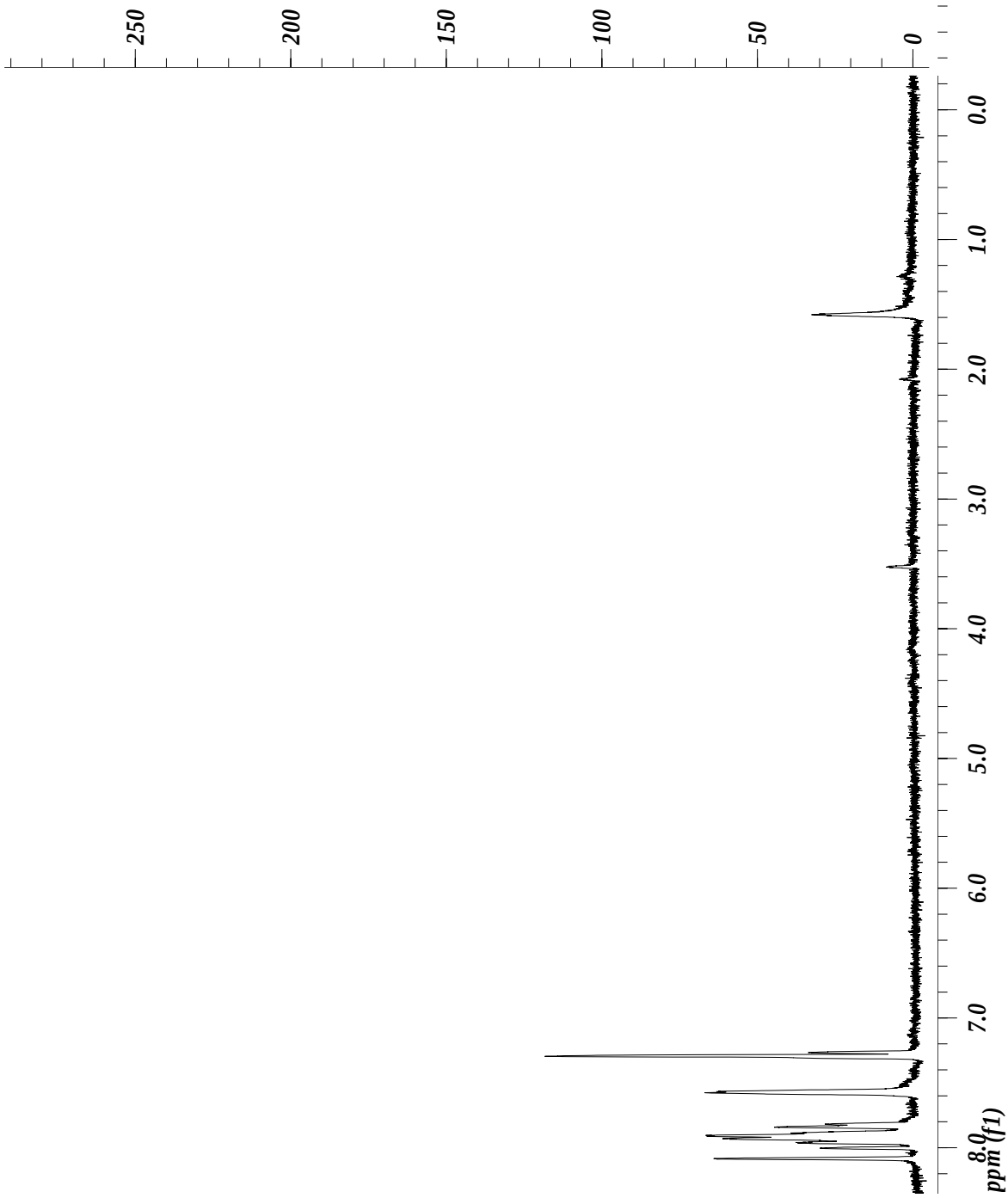

1,5-Di(napthalen-1-yl)penta-1,4-dien-3-one

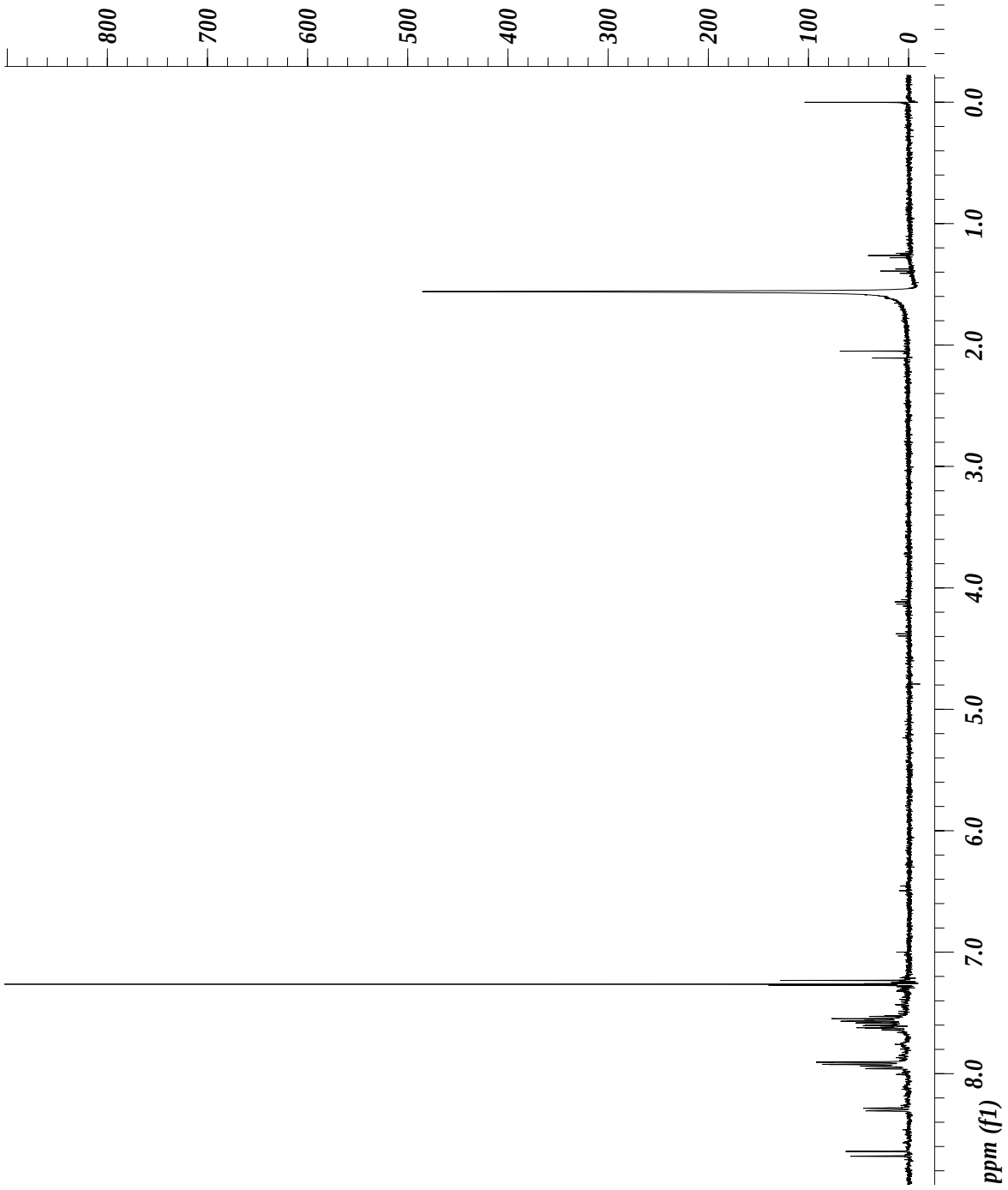

2,6-Di(2-chloro-6-fluorobenzylidene)cyclohexanone

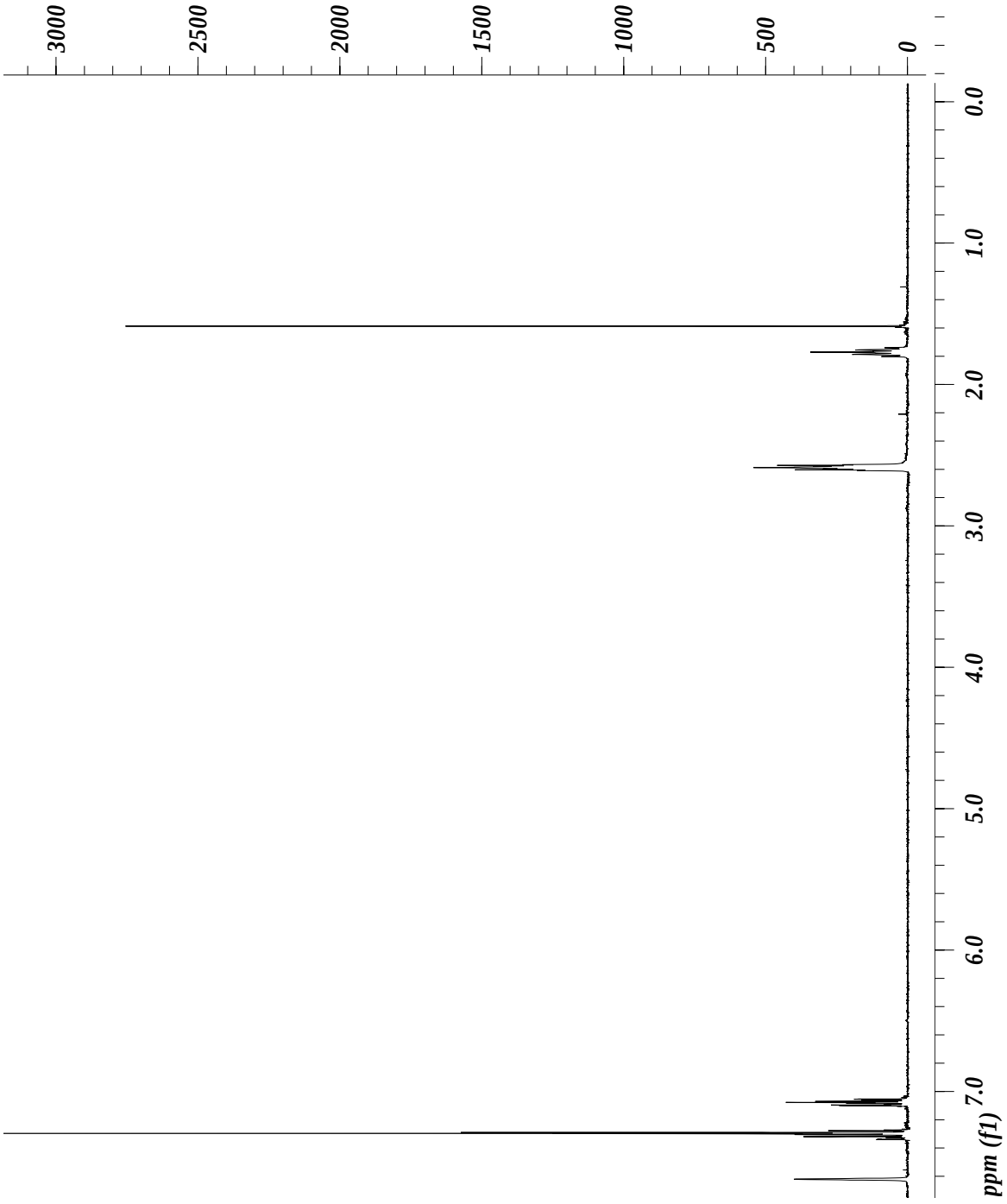

1,5-Di(anthracen-9-yl)penta-1,4-dien-3-one

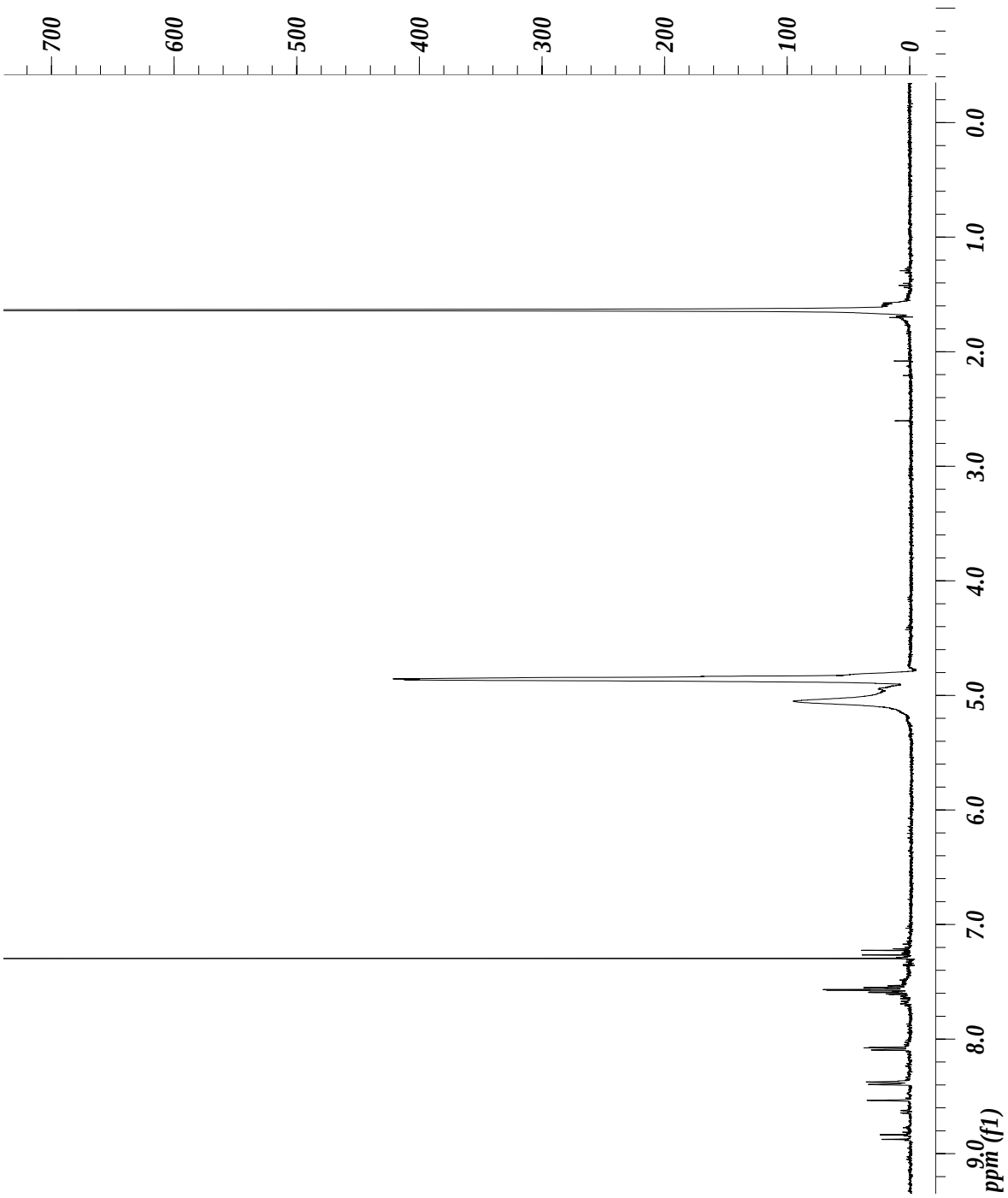

2,6-Di(anthracen-9-ylmethylene)cyclohexanone

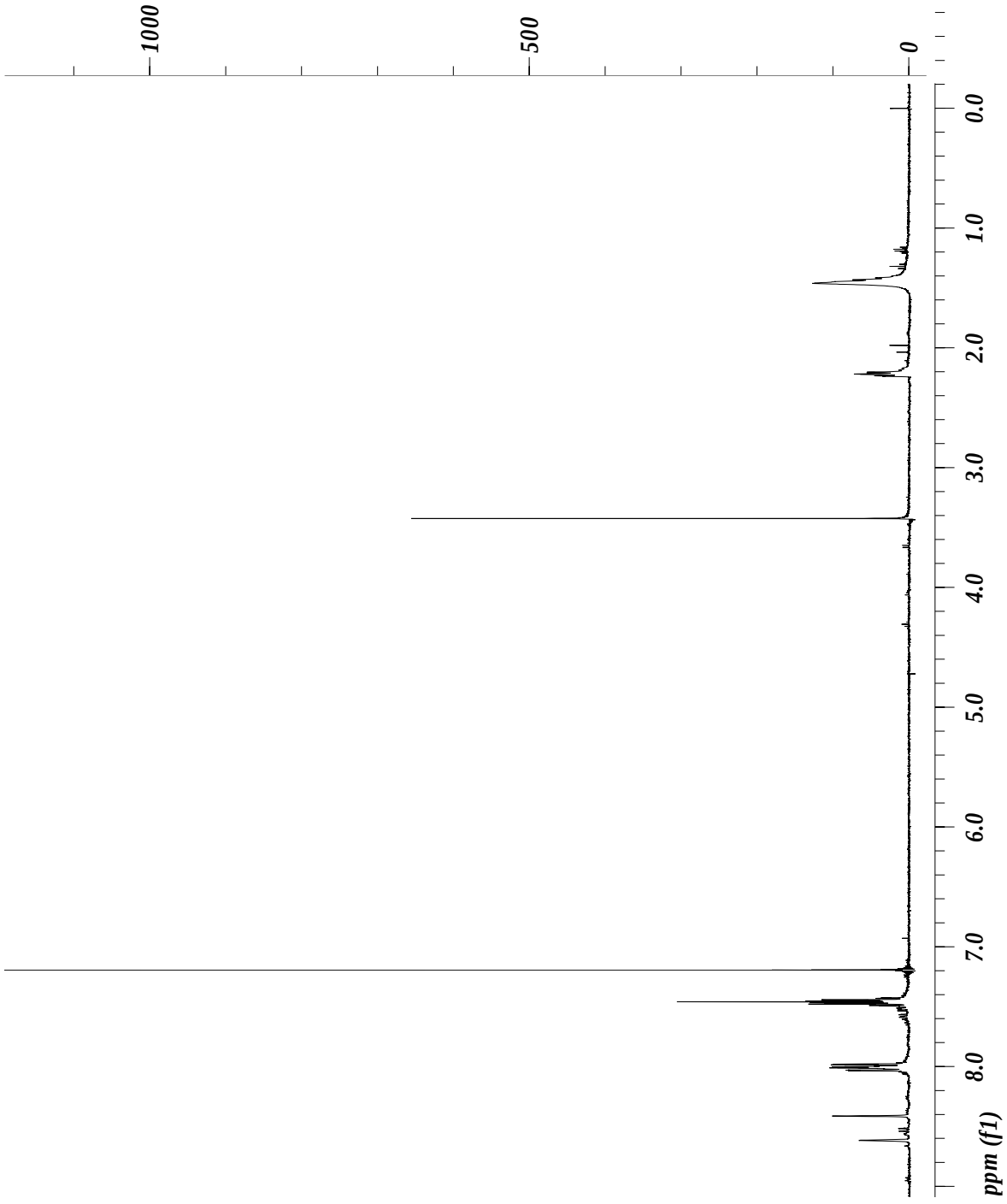

1,5-Diphenyl-1,4-dien-3-one

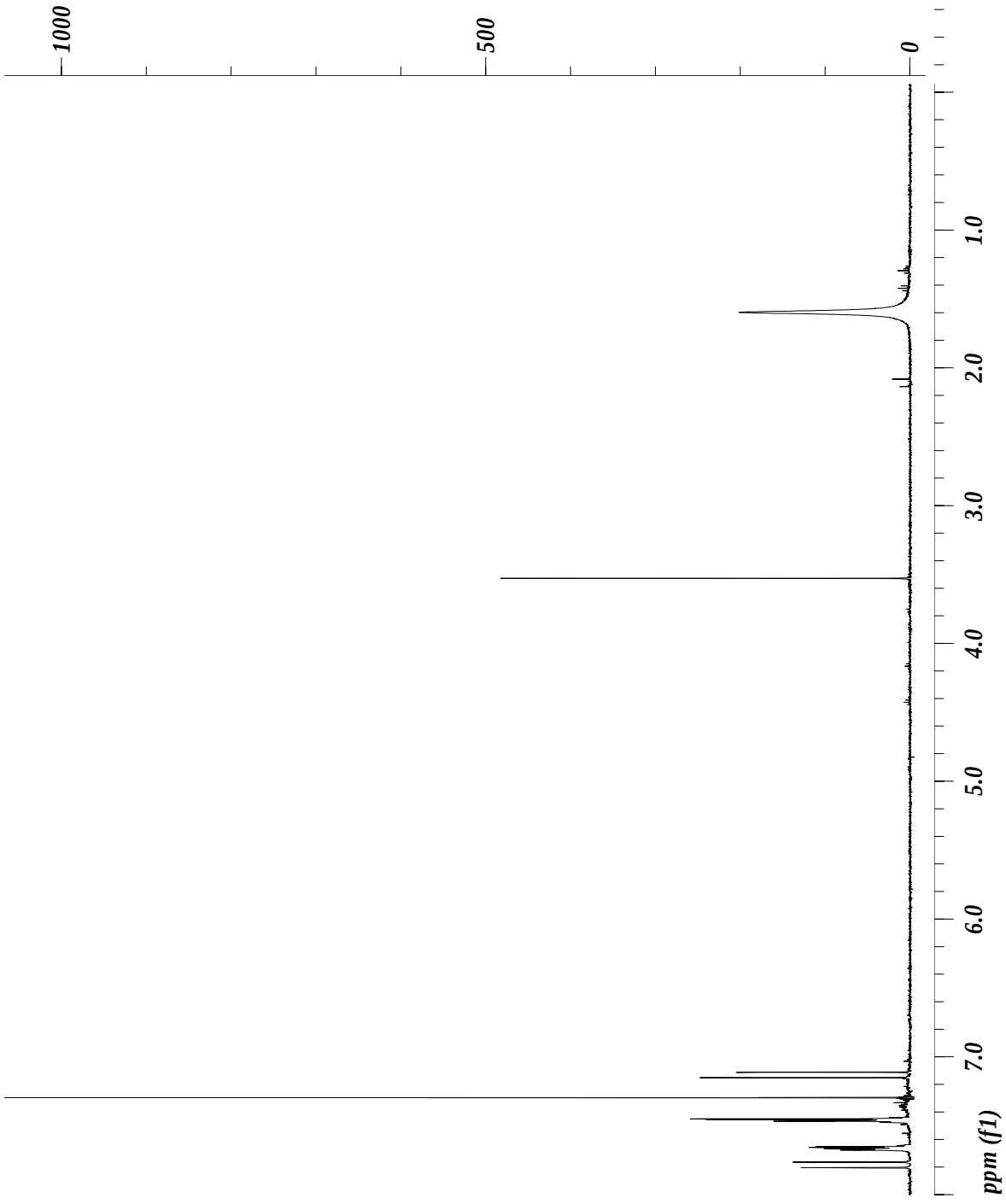

(4-Allyloxyphenyl)-(2-allyloxyphenyl)methanone